CIMNE
International Centre
for Numerical Methods in Engineering

UNIVERSITAT POLITÈCNICA
DE CATALUNYA
BARCELONATECH

DEM CONTACT FORCE MODELS

Rafael Rangel
(rrangel@cimne.upc.edu)

Date: July 2021

DOI: 10.5281/zenodo.13846092

Summary

1 – Introduction

Continuum vs. Discrete

Two modeling approaches are commonly used for granular media

Continuum

Constitutive laws are employed to relate stress and strain / strain rate

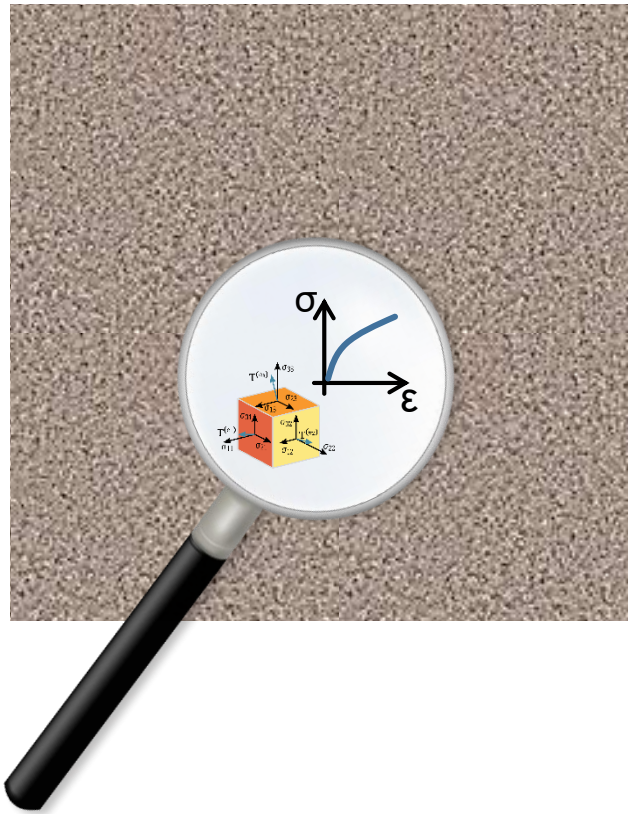

Discrete

The macroscopic behavior results from the individual particle interactions

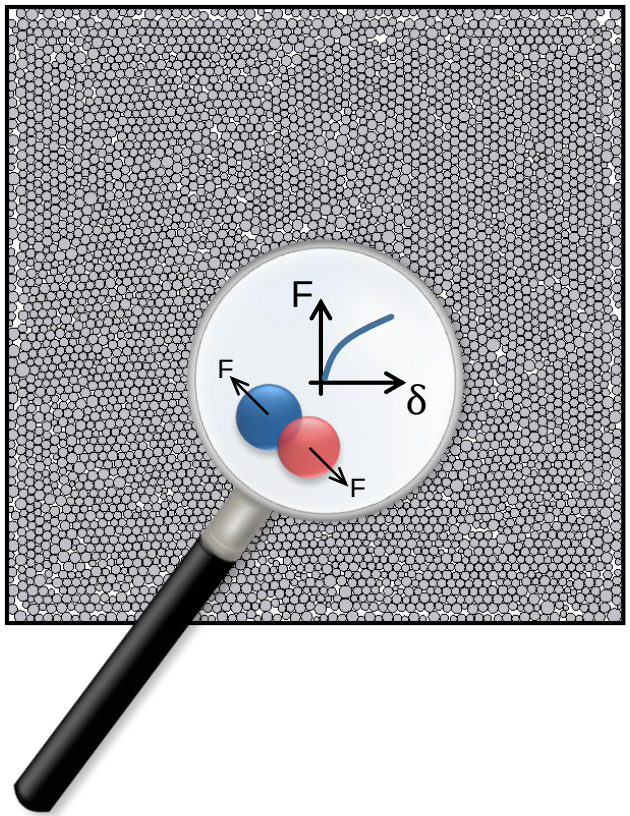

Hard-Sphere vs. Soft-Sphere

Two types of simulation are commonly used within the discrete approach

Hard-Sphere

- Interaction forces are impulsive and not explicitly considered.
- Particles only exchange momentum through collision.
- Binary (pairwise) collisions only.
- Event-driven time steps: contact is instantaneous.
- Efficient for dilute systems: when the time between collisions is much larger than the collision duration.

Soft-Sphere

- Small overlaps are allowed to represent deformations during contact.
- Multiple contacts can happen simultaneously.
- Contact duration is finite and happens over several time steps.
- More time consuming due to smaller time steps.
- Most accurate and common approach for dense systems.

In both approaches, the geometry of particles is maintained during and after contacts.

Many shapes can be used, but spheres are the most common due to simplicity.

Focus here on soft-sphere-shaped particles!

Time Step Calculation Cycle

DEM = Newton's 2nd law + Contact Mechanics

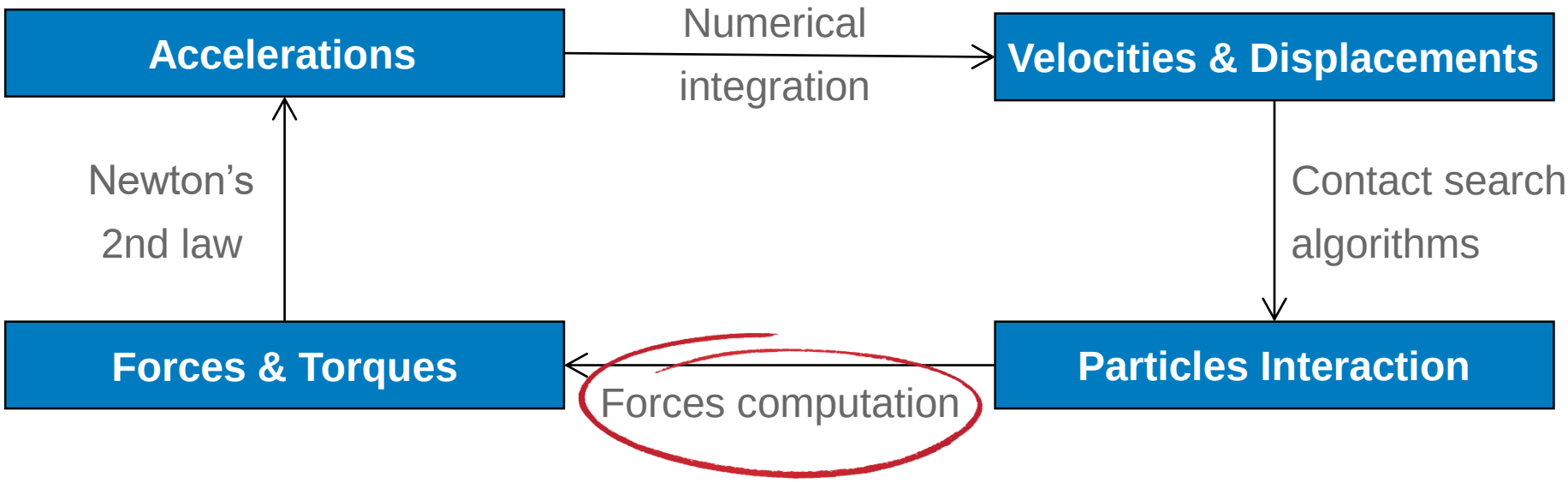

Forces Acting on a Particle

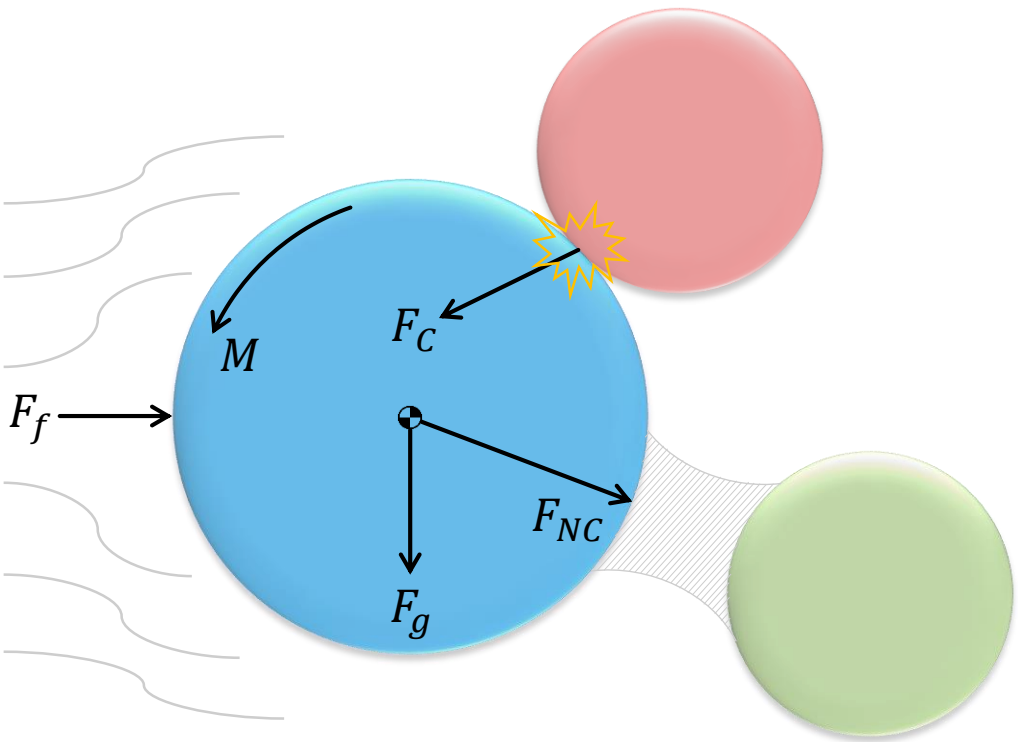

F_C → **Contact forces** with particles/walls: Deformation of particle surface due to mechanical contact.

F_{NC} → **Non-contact forces**: Cohesion (e.g. liquid bridging), electrostatics, Van der Waals, etc.

F_g → **Gravitational force** (weight): Acts on the center of mass and does not cause rotation.

F_f → **Fluid forces**: Occur in multiphase flows (drag, buoyancy, lift, etc.).

M → **Torque**: Resultant torque from forces eccentricities and rolling resistance.

The resulting force / torque acting on a particle at any time step is given by the sum of the pairwise interaction with all other particles or walls.

Contact Forces

- Particles deformation during collision is represented as overlaps.
- Limited to small overlaps: contact area much smaller than the radii of spheres.
- Normal and tangential overlaps are considered, leading to forces in these directions.
- Normal forces (F_n) cause change of translational motion;
  Tangential forces (F_t) cause changes of rotational motion.

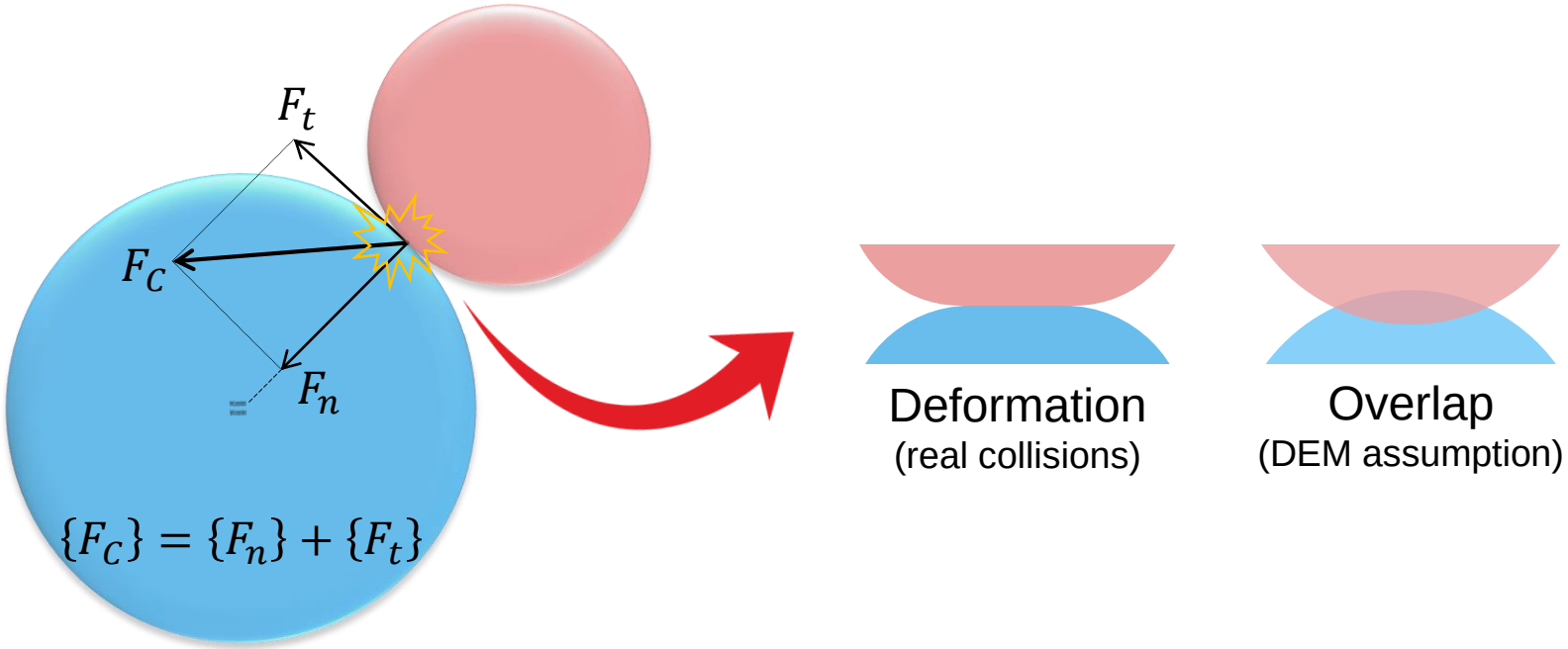

Contact Force Models

Contact force models relate the amount of overlaps with the magnitude of forces.

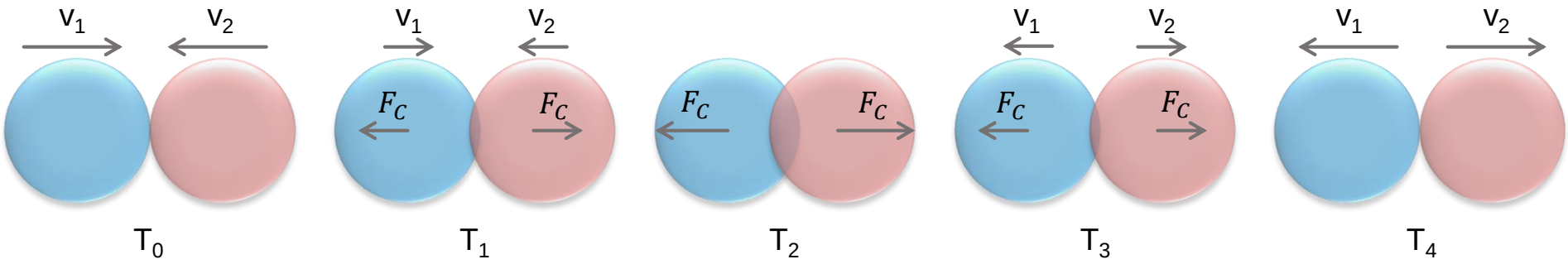

Mechanical contact:
Normal overlap (δ_n)>0

Approach / loading ⟷ Separation / unloading

Detachment

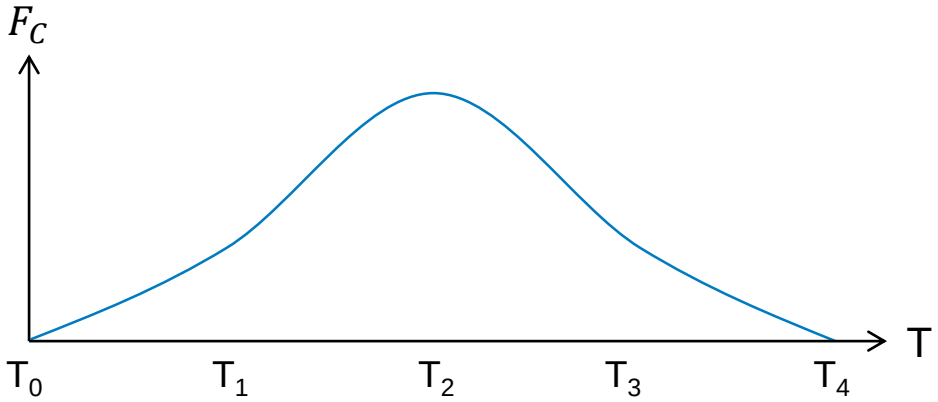

Contact Force Models

There are several models capable of simulating linear and nonlinear elastic, viscoelastic, elastoplastic and viscoplastic collisions by employing conservative and dissipative mechanical elements between particles, in normal and tangential directions, such as:

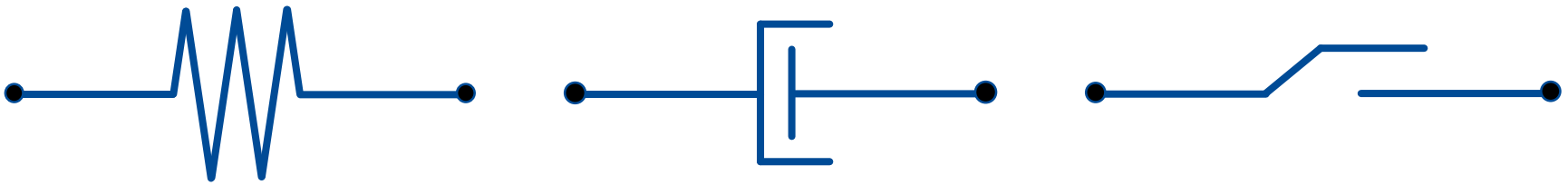

Spring
(elastic force)

Dashpot
(damping/viscous force)

Slider
(friction force)

The force-displacement law is a function of the material parameters, amount of overlaps, relative velocity, and contact history.

There are way too many contact models and only some basic and common ones will be presented here.

2 – Contact Kinematics

Contact Kinematics

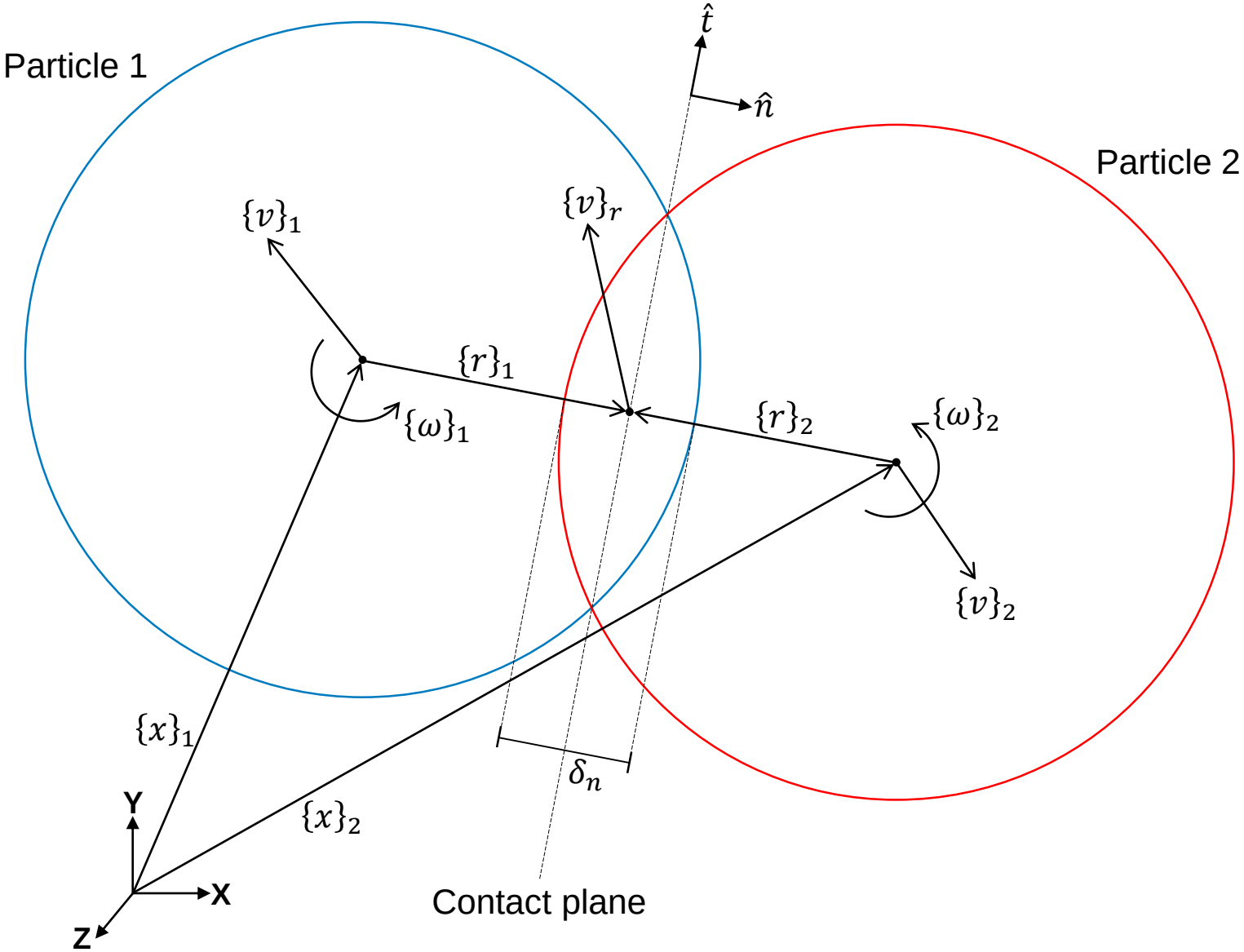

Contact Kinematics

Lengths & Positions

Distance between spheres:

$$d = |\{x\}_2 - \{x\}_1|$$

Overlaps:

$$\delta_n = (R_1 + R_2) - d$$

$$\delta_t = \int_{T_0}^{T} \dot{\delta}_t dT \cong \sum_{T_0}^{T} \Delta\delta_t \rightarrow \Delta\delta_t = \dot{\delta}_t . \Delta T$$

Unit vectors:

$$\hat{n} = (\{x\}_2 - \{x\}_1)/d$$

$$\hat{t} = \{v\}_r^t / |\{v\}_r^t|$$

Position of contact point:

$$\{r\}_1 = (R_1 - \delta_n/2)\hat{n}$$

$$\{r\}_2 = -(R_2 - \delta_n/2)\hat{n}$$

Velocities

Particle velocities at contact point:

$$\{v\}_{r1} = \{v\}_1 + \{\omega\}_1 \times \{r\}_1$$

$$\{v\}_{r2} = \{v\}_2 + \{\omega\}_2 \times \{r\}_2$$

Relative velocity at contact point:

$$\{v\}_r = \{v\}_{r1} - \{v\}_{r2} = \{v\}_r^n + \{v\}_r^t$$

Relative velocity components:

$$\{v\}_r^n = (\{v\}_r \cdot \hat{n})\hat{n} = \dot{\delta}_n \hat{n}$$

$$\{v\}_r^t = (\{v\}_r \cdot \hat{t})\hat{t} = \dot{\delta}_t \hat{t}$$

$$\{v\}_r^t = \{v\}_r - \{v\}_r^n$$

$$\dot{\delta}_n = \{v\}_r \cdot \hat{n}$$

$$\dot{\delta}_t = \{v\}_r \cdot \hat{t}$$

Contact Kinematics

Effective Parameters for the Collision of 2 Spheres

$$\bar{R} = \left(\frac{1}{R_1} + \frac{1}{R_2}\right)^{-1} = \frac{R_1 \cdot R_2}{(R_1 + R_2)}$$

$$\bar{m} = \left(\frac{1}{m_1} + \frac{1}{m_2}\right)^{-1} = \frac{m_1 \cdot m_2}{(m_1 + m_2)}$$

$$\bar{E} = \left(\frac{1 - (\upsilon_1)^2}{E_1} + \frac{1 - (\upsilon_2)^2}{E_2}\right)^{-1}$$

$$\bar{G} = \left(\frac{2 - \upsilon_1}{G_1} + \frac{2 - \upsilon_1}{G_2}\right)^{-1}$$

Collision with a rigid wall:

$$R_{\text{wall}} = m_{\text{wall}} = E_{\text{wall}} = G_{\text{wall}} = \infty$$

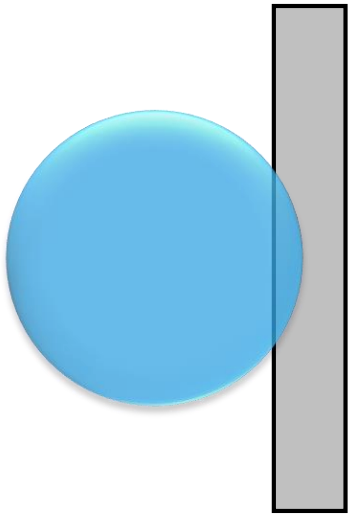

3 – Normal Force

Coefficient of Restitution

The restitution coefficient measures the velocity decrease of a particle before and after a collision.

$$\varepsilon_n = \left| \frac{\dot{\delta}_n^{reb}}{\dot{\delta}_n^0} \right|$$

→ Normal relative velocity after collision (rebound)

→ Normal relative velocity before collision (impact velocity)

It consists on the fraction of kinetic energy recovered during collision.

Perfectly elastic collision: $\varepsilon_n = 1$

Perfectly inelastic collision: $\varepsilon_n = 0$

Real collisions: $0 < \varepsilon_n < 1$

It is usually a basic property of a particle, and can be measured experimentally with a simple free-fall test:

$$\varepsilon_n = \sqrt{\frac{h_{reb}}{h_0}}$$

→ Max. height after rebound

→ Height of drop

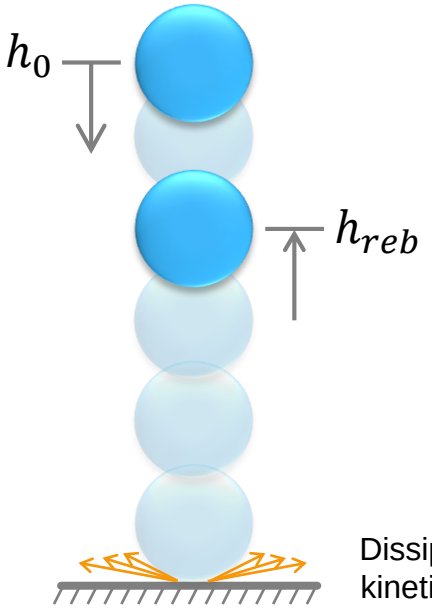

Dissipation of kinetic energy:

Thermal energy, elastic waves (sound), viscoelasticity, plastic deformations, etc.

Viscoelastic Model

The collision force consists of a conservative and a dissipative component.

Elastic Force (F_n^{el}):

- Simulated by a spring.
- A function (linear or not) of the normal overlap, given by a stiffness coefficient.
- Repulsive force that provides elastic rebound.
- Conserves the kinetic energy of collision.

Viscous Force (F_n^{vis}):

- Simulated by a dashpot.
- A function (linear or not) of the relative normal velocity, given by a damping coefficient.
- Resisting force against the motion.
- Dissipates the kinetic energy of collision.

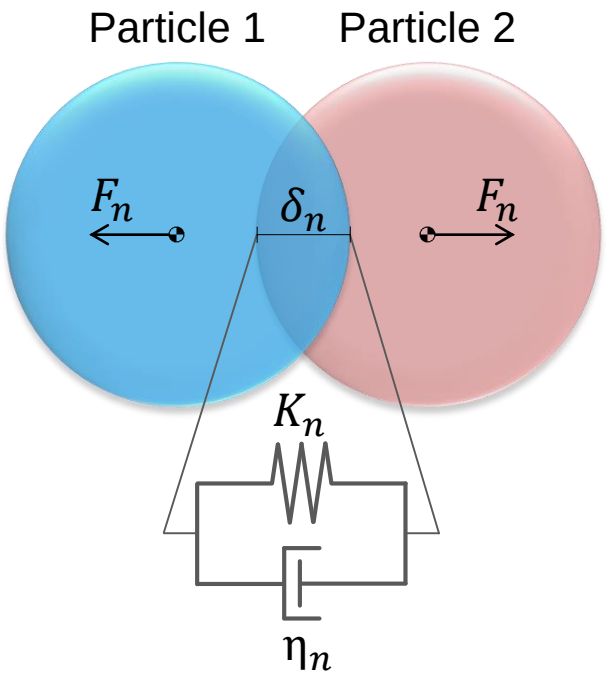

K_n → Normal spring stiffness

η_n → Normal damping coeff.

Force on particle 1:

$$\{F_n\} = -\left(F_n^{el} + F_n^{vis}\right)\hat{n}$$

Viscoelastic Model

Remarks on viscoelastic models:

- **Little energy dissipation for quasi-static systems**:
  The reason is that the dissipative term is a velocity-dependent viscous force.

- **Reduction of spring stiffness**:
  It is common to use a stiffness value smaller than the real one in order to increase the contact duration, so a larger time step can be used (less costly simulation). Although it can provide good results, care must be taken as the stiffness affects the magnitude of overlaps / forces and can lead to unrealistic results.

  E.g. soft springs can make the solid fraction above 1.0 in compressed systems, and provide overlaps so large that the small deformation assumption is not valid, causing modeling errors due to the excluded volume effect.

- **Unrealistic cohesive force**:
  During the separation stage ($\delta_n > 0$ and $\dot{\delta}_n < 0$), towards the end of the impact, it is possible that the viscous force (proportional to $\dot{\delta}_n$) exceeds the elastic force (proportional to δ_n), resulting in a total force that is attractive, which is non-realistic.

Viscoelastic Model

- **Reduction collision time**:
  Physically, the unrealistic attractive force means that the separation of particles is occurring so fast that the deformation cannot recover at the same speed. Therefore, although an overlap is considered, the particles do not touch anymore and the velocity should not change.

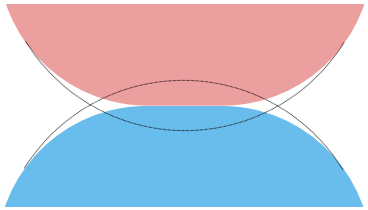

Contact with deformation and DEM overlap

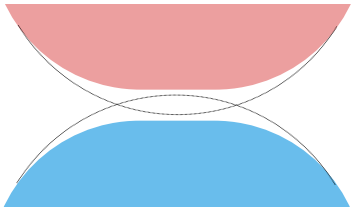

No contact with deformation and DEM overlap

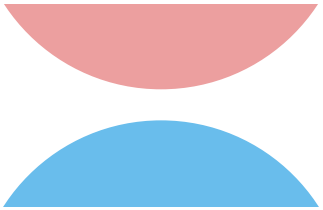

No contact with no deformation nor DEM overlap

A consequence of the unrealistic attractive force is that particles separate at a lower velocity. An overcome to consider the reduction collision time is to always limit the total force value to a positive value (Poschel & Schwager, 2005):

$$F_n^{el} + F_n^{vis} \geq 0$$

Viscoelastic Model – Linear

Normal Linear Spring-Dashpot (LSDn)

Both elastic and viscous forces are a linear function of the normal overlap and the relative normal velocity, respectively:

$$\begin{cases} F_n^{el} = K_n \delta_n \\ F_n^{vis} = \eta_n \dot{\delta}_n \end{cases}$$

Equation of motion for a particle collision: $\bar{m}\ddot{\delta}_n + \eta_n \dot{\delta}_n + K_n \delta_n = 0$

Initial conditions: $\begin{cases} \delta_n(0) = 0 \\ \dot{\delta}_n(0) = \dot{\delta}_n^0 \end{cases}$

Solution:
(Analytical!)

$$\begin{cases} \delta_n(T) = \dfrac{\dot{\delta}_n^0}{W} e^{-\Psi T} \sin(WT) \\ \dot{\delta}_n(T) = \dfrac{\dot{\delta}_n^0}{W} e^{-\Psi T} (W \cos(WT) - \Psi \sin(WT)) \end{cases}$$

Auxiliary parameters:

$$\Psi = \eta_n / 2\bar{m}$$

$$\Phi = \sqrt{K_n / \bar{m}}$$

$$W = \sqrt{\Phi^2 - \Psi^2}$$

$$\beta = \pi / \ln(\varepsilon_n)$$

*Proposed by Cundall & Strack (1979)

Viscoelastic Model – Linear

Collision duration: $\delta_n(T_c) = 0 \rightarrow \frac{\dot{\delta}_n^0}{W} e^{-\Psi T_c} \sin(W T_c) = 0 \rightarrow W T_c = \pi \rightarrow T_c = \frac{\pi}{W}$

$$T_c = \frac{\pi}{\sqrt{K_n/\bar{m} - \eta_n{}^2/4\bar{m}^2}} \qquad \text{or also} \qquad T_c = \pi \sqrt{\frac{\bar{m}}{K_n}\left(1 + \frac{1}{\beta^2}\right)}$$

Rebound velocity: $\dot{\delta}_n^{reb} = \dot{\delta}_n(T_c) = \frac{\dot{\delta}_n^0}{W} e^{-\Psi T_c}(W \cos(W T_c) - \Psi \sin(W T_c)) = \dot{\delta}_n^0 e^{-\Psi T_c}$

$$\dot{\delta}_n^{reb} = \dot{\delta}_n^0 \exp\left(-\frac{\eta_n \pi}{2\bar{m}\sqrt{K_n/\bar{m} - \eta_n{}^2/4\bar{m}^2}}\right)$$

Maximum overlap:

$$\delta_n^{max} = \dot{\delta}_n^0 \sqrt{\frac{\bar{m}}{K_n}} \exp\left(-\frac{\tan^{-1}(\beta)}{\beta}\right)$$

Viscoelastic Model – Linear

Damping coefficient:

The coefficient of restitution is expressed in terms of the damping coefficient (inversely proportional – $\varepsilon_n \downarrow$ as $\eta_n \uparrow$):

$$\varepsilon_n = \left| \frac{\dot{\delta}_n^{reb}}{\dot{\delta}_n^0} \right| = \exp\left(- \frac{\eta_n \pi}{2\bar{m}\sqrt{K_n/\bar{m} - {\eta_n}^2/4\bar{m}^2}} \right)$$

Since the coefficient of restitution is a given particle property, the damping coefficient is obtained in terms of it by rearranging the previous equation:

$$\eta_n = -\frac{2\ln(\varepsilon_n)\sqrt{\bar{m}K_n}}{\sqrt{\ln(\varepsilon_n)^2 + \pi^2}} \qquad \text{or also} \qquad \eta_n = \sqrt{\frac{4\bar{m}K_n}{(1+\beta^2)}}$$

P.S.: When the collision time reduction is applied, a slightly larger restitution coefficient is obtained and it should be considered in the derivation of the equations.

Viscoelastic Model – Linear

Spring stiffness coefficient:

There are many methods to determine the spring stiffness and a general method is not widely agreed upon.

3 methods will be presented, each one sets a particular parameter equal to the respective result obtained with the NSDn model.

1) Equivalent Collision Duration:

LSDn: $T_c = \pi \sqrt{\frac{\bar{m}}{K_n}\left(1 + \frac{1}{\beta^2}\right)}$

NSDn: $T_c = 2.870 \left(\frac{\bar{m}^2}{\dot{\delta}_n^0 \bar{R} \bar{E}^2}\right)^{1/5}$

Equalizing and rearranging the terms:

$$K_n \cong 1.198 \left(\dot{\delta}_n^0 \bar{R} \bar{E}^2 \sqrt{\bar{m}}\right)^{2/5} \left(1 + \frac{1}{\beta^2}\right)$$

Viscoelastic Model – Linear

2) Equivalent Maximum Overlap:

LSDn: $\delta_n^{max} = \dot{\delta}_n^0 \sqrt{\frac{\bar{m}}{K_n}} \exp\left(-\frac{\tan^{-1}(\beta)}{\beta}\right)$

NSDn: $\delta_n^{max} = \left(\frac{15}{16}\frac{\bar{m}}{\sqrt{\bar{R}}\bar{E}}\left(\dot{\delta}_n^0\right)^2\right)^{2/5}$

$$K_n \cong 1.053\left(\dot{\delta}_n^0 \bar{R}\bar{E}^2\sqrt{\bar{m}}\right)^{2/5}\left(\exp\left(-\frac{\tan^{-1}(\beta)}{\beta}\right)\right)^2$$

3) Equivalent Maximum Strain Energy:

LSDn: $\frac{1}{2}K_n(\delta_n^{max})^2$

NSDn: $\frac{2}{5}K_{HZ}(\delta_n^{max})^{5/2}$

$$K_n \cong 1.053\left(\dot{\delta}_n^0 \bar{R}\bar{E}^2\sqrt{\bar{m}}\right)^{2/5}$$

Viscoelastic Model – Linear

Graphs aspect for different values of the restitution coefficient:

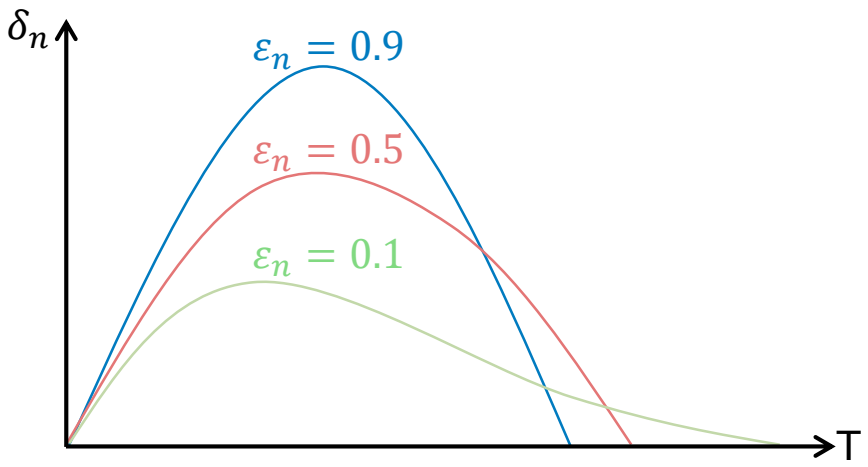

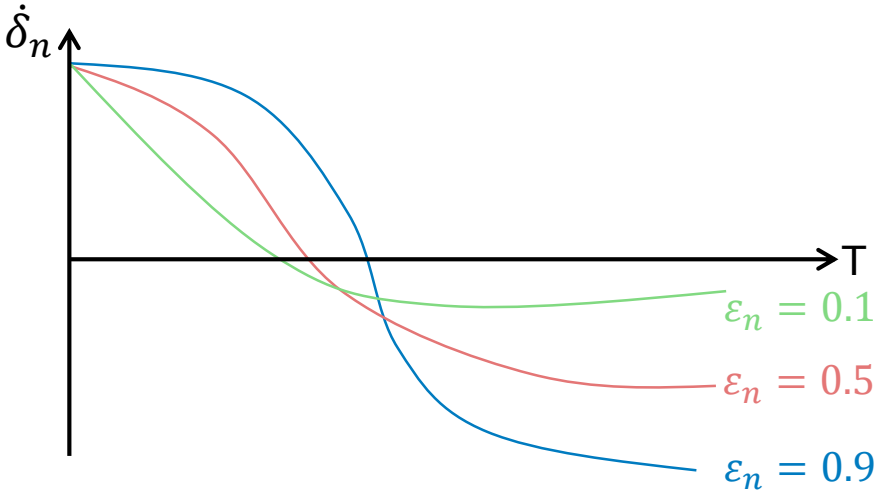

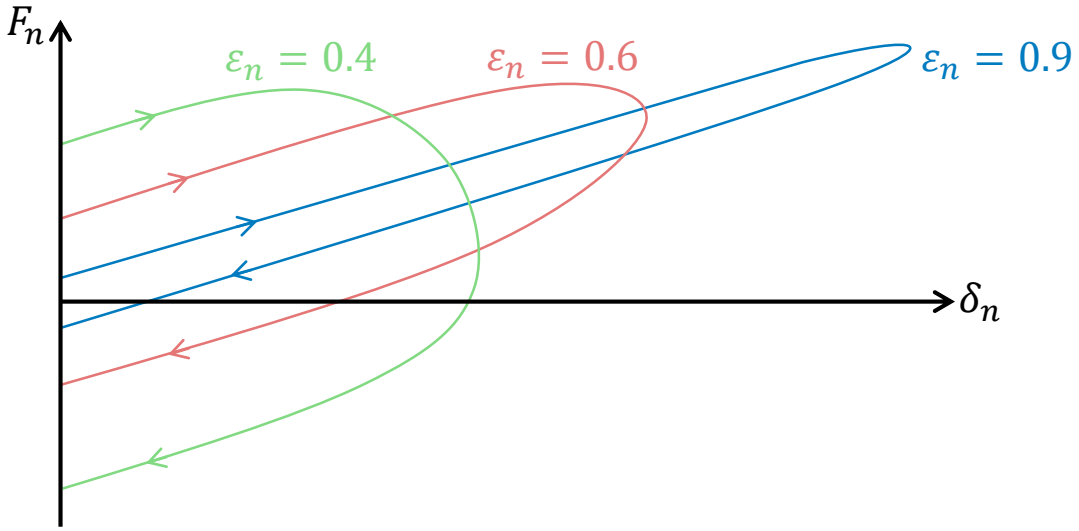

Loading and unloading curves are not the same due to viscous dissipation (energy dissipation is the area between these curves).

The maximum overlap of the particle decreases and the distance between loading and unloading curves becomes broader with increasing the damping coefficient.

Viscoelastic Model – Linear

Remarks on the LSDn model:

- **Advantages**:
  Simple model; easy to implement; widely used; relies on analytical solution.
- **Independency on impact velocity**:
  Restitution coefficient and collision duration are independent of the impact velocity.
  However, in real collisions: $\dot{\delta}_n^0 \uparrow$ makes $\varepsilon_n \downarrow$ and $T_c \downarrow$.
- **Discontinuous force**:
  The contact force is non-zero at the start / end of the contact due to the viscous dissipation, which occurs because the relative velocity is not zero when particles touch / detach.
  However, in real collisions the forces are continuous at the start / end of the contact (there are remedies to overcome this behavior but with limitations).
- **Parameters behavior**:
  $T_c \uparrow$ as $K_n \downarrow$, $\bar{m} \uparrow$, $\varepsilon_n \downarrow$, $\eta_n \uparrow$
  $\delta_n^{max} \uparrow$ as $\dot{\delta}_n^0 \uparrow$, $K_n \downarrow$, $\bar{m} \uparrow$, $\varepsilon_n \downarrow$, $\eta_n \uparrow$

Viscoelastic Model – Nonlinear

Normal Nonlinear Spring-Dashpot (NSDn)

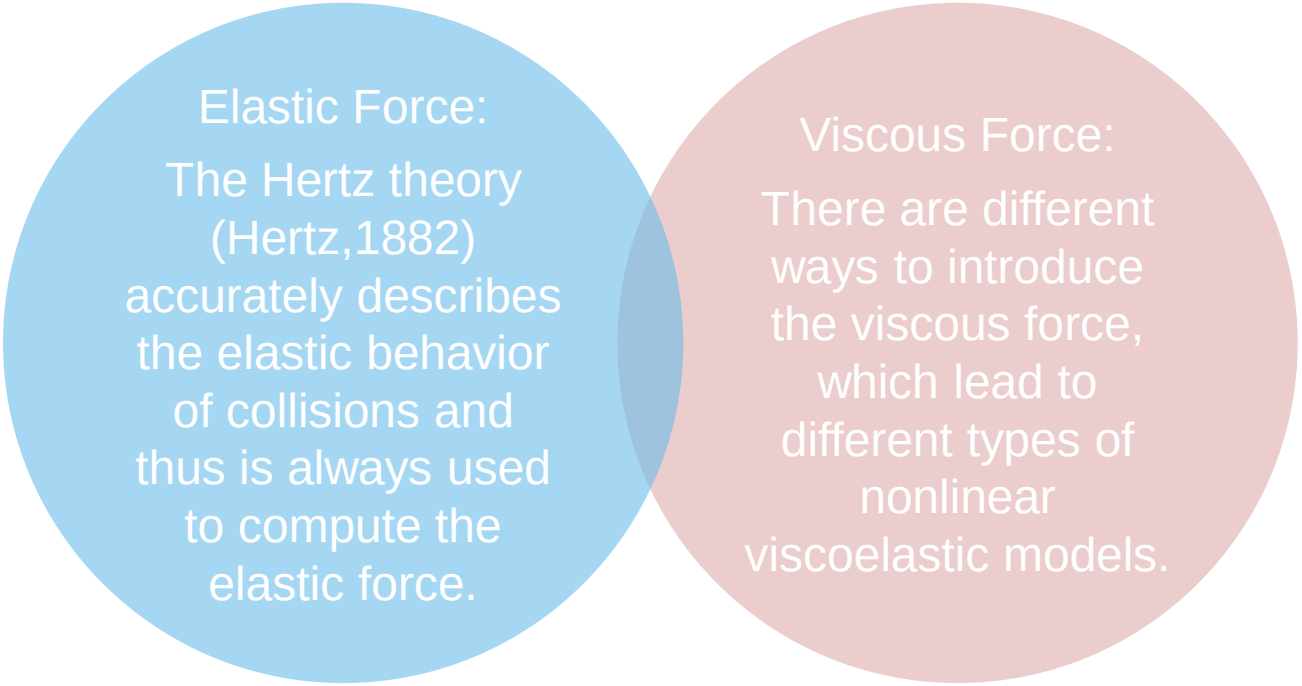

The NSDn model has a higher accuracy than the LSDn model and is in better agreement with experimental results.

Viscoelastic Model – Nonlinear

Nonlinear elastic force:

The Hertzian contact is based on the linear theory of elasticity (Johnson, 1985).

Considering a perfectly elastic and smooth sphere compressed against a frictionless rigid wall with a force F_n^{el}, it is possible to compute the stress distribution, $P_{(r)}$, and the contact geometry in order to find the relation between F_n^{el} and δ_n.

The contact area is circular, with radius a, and it predicts an axisymmetric distribution of normal stress over the contact area as a function of the radial coordinate *r*.

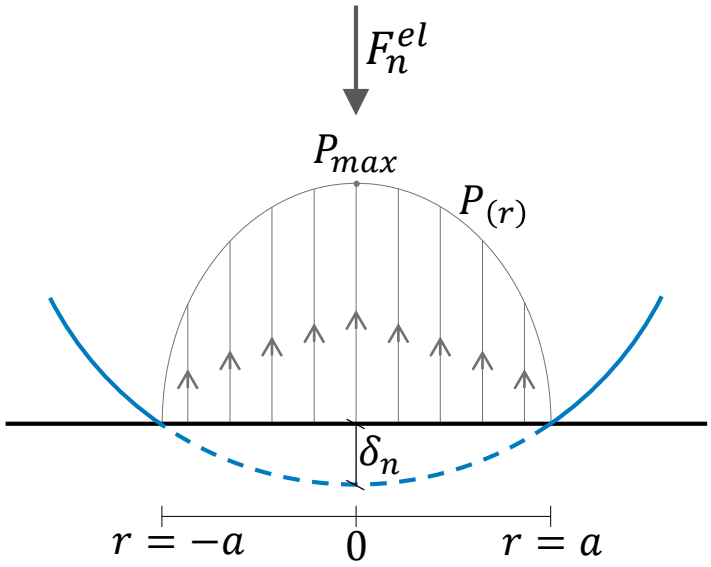

Normal pressure distribution:

$$P_{(r)} = P_{max}\sqrt{1 - \left(\frac{r}{a}\right)^2}$$

$$P_{max} = \frac{3F_n^{el}}{2\pi a^2} = \left(\frac{6F_n^{el}\bar{E}^2}{\pi^3\bar{R}}\right)^{1/3}$$

Viscoelastic Model – Nonlinear

From the equation of maximum pressure, the radius of the contact area, and subsequently the normal overlap, are obtained:

$$a = \left(\frac{3}{4} \frac{F_n^{el} \bar{R}}{\bar{E}} \right)^{1/3}$$

$$\delta_n = \frac{a^2}{\bar{R}} = \left(\frac{9}{16} \frac{{F_n^{el}}^2}{\bar{R} \bar{E}^2} \right)^{1/3}$$

Rearranging the terms of the last equation, it is possible to find the relation between the elastic normal force and the normal overlap:

$$F_n^{el} = K_{HZ} {\delta_n}^{3/2} \qquad K_{HZ} = \frac{4}{3} \bar{E} \sqrt{\bar{R}}$$

We note that the Hertz contact force does not depend linearly on the overlap, although the bodies are elastic. This is due to the increase of the contact area as the force increases, which increases the effective stiffness

Viscoelastic Model – Nonlinear

Solving for a purely elastic collision (no viscous force included yet):

Equation of motion for a particle collision: $\bar{m}\ddot{\delta}_n + K_{HZ}{\delta_n}^{3/2} = 0$

Initial conditions: $\begin{cases} \delta_n(0) = 0 \\ \dot{\delta}_n(0) = \dot{\delta}_n^0 \end{cases}$

Collision duration: $T_c \cong 2.86\left(\frac{\bar{m}^2}{\dot{\delta}_n^0 \bar{R}\bar{E}^2}\right)^{1/5}$

Maximum overlap: $\delta_n^{max} = \left(\frac{15}{16}\frac{\bar{m}}{\sqrt{\bar{R}}\bar{E}}\left(\dot{\delta}_n^0\right)^2\right)^{2/5}$

The force-displacement curves are considerably different from real collisions.

However, The collision duration is now an inverse function of the impact speed (in the linear model they were not related), so the collision duration is closer to experiments.

Viscoelastic Model – Nonlinear

Nonlinear viscous force:

There are different ways to introduce the velocity-dependent energy dissipation, which lead to different types of nonlinear viscoelastic models. A few of them will be shown.

In most of them, the value of damping coefficient is usually obtained by experiments or calibrated to fit experimental results.

1) BSHPn Model:

Proposed by Brilliantov et. al (1996).

$$F_n^{vis} = \frac{4}{3}\bar{E}\sqrt{\bar{R}}\bar{A}(\delta_n)^{1/2}\dot{\delta}_n$$

where *A* is a dissipative constant that depends on the material viscosity and can be obtained experimentally.
For 2 particles with different materials, Poschel & Schwager (2005) suggest to use the arithmetic mean of *A* as the effective dissipative constant:

$$\bar{A} = (A_1 + A_2)/2$$

Viscoelastic Model – Nonlinear

2) KKn Model:

Proposed by Kuwabara & Kono (1987).

$$F_n^{vis} = \eta_n(\delta_n)^{1/2}\dot{\delta}_n$$

The value of the damping coefficient is usually calibrated to fit experimental results.

Equivalent to the previous model by taking: $\eta_n = \frac{4}{3}\bar{E}\sqrt{\bar{R}}\bar{A}$

---

3) TTIn Model:

Proposed by Tsuji et. al (1992).

$$F_n^{vis} = \eta_n(\delta_n)^{1/4}\dot{\delta}_n$$

An expression for the damping coefficient is proposed by Norouzi et. al (2016), which is a correlation based on experimental data:

$$\eta_n = -2.2664\frac{\ln(\varepsilon_n)\sqrt{\bar{m}K_{HZ}}}{\sqrt{(\ln(\varepsilon_n))^2 + 10.1354}}$$

Viscoelastic Model – Nonlinear

Graphs aspect for different values of the restitution coefficient:

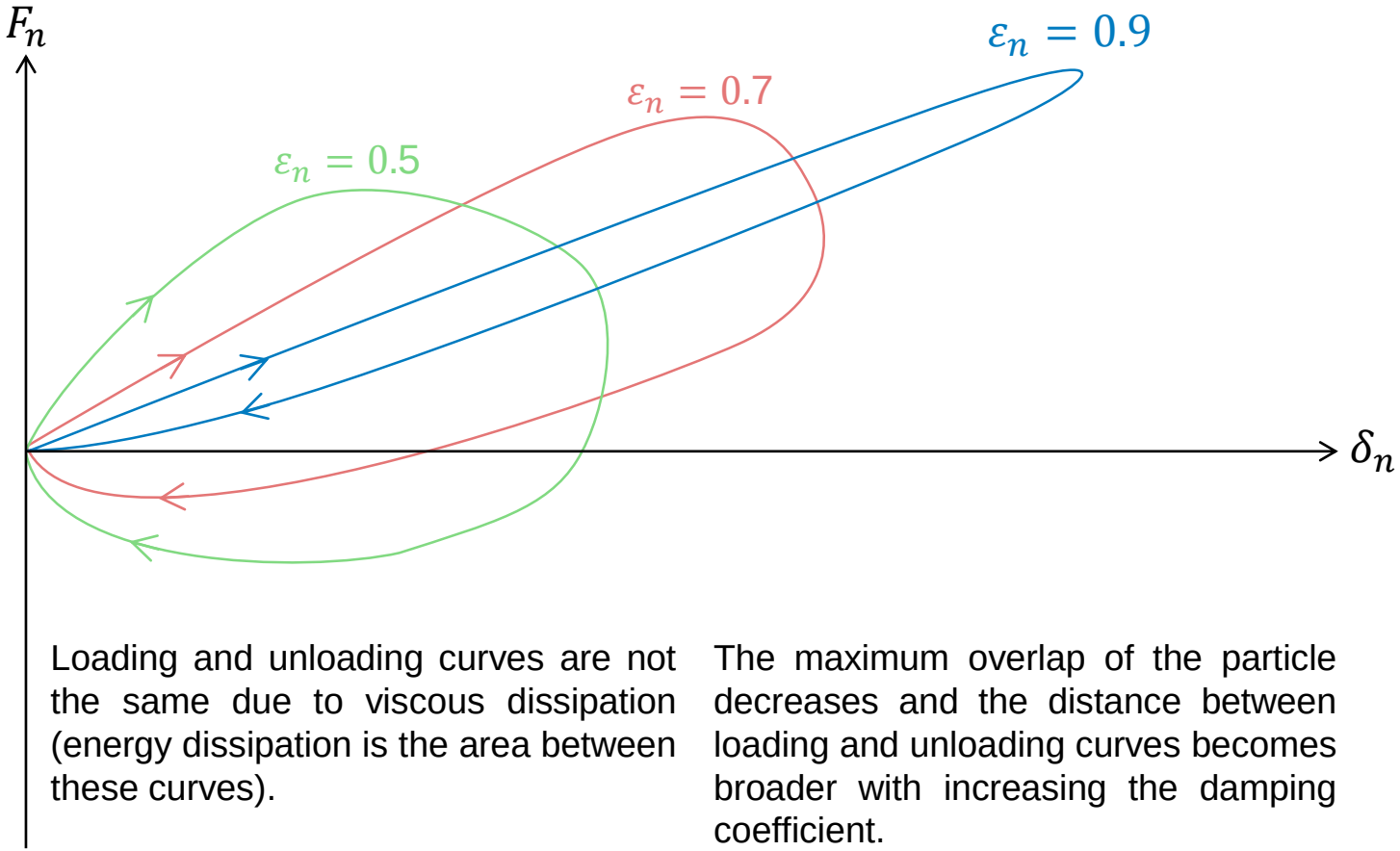

Loading and unloading curves are not the same due to viscous dissipation (energy dissipation is the area between these curves).

The maximum overlap of the particle decreases and the distance between loading and unloading curves becomes broader with increasing the damping coefficient.

Viscoelastic Model – Nonlinear

Remarks on the NSDn model:

- **Dependency on impact velocity:**
  The collision duration is an inverse function of the impact velocity, which is an improvement relative to the LSDn model.
- **Continuous force:**
  The normal force is zero at the start / end of contact for all values of the restitution coefficient, which is an improvement relative to the LSDn model and is in agreement with real collisions.
- **Cohesive force:**
  As in the LSDn model, the force is cohesive towards the end of the impact, due to the collision time reduction.

Elastic Perfectly Plastic Model

Hysteric Linear Spring (HLS)

- **Energy dissipation due to spring hysteresis**:
  The spring stiffness adopts different values depending on whether particles approach or depart from each other.
- **Elastic perfectly plastic model**:
  The hysteretic stiffness behavior models the strain hardening of the material due to plastic deformation.

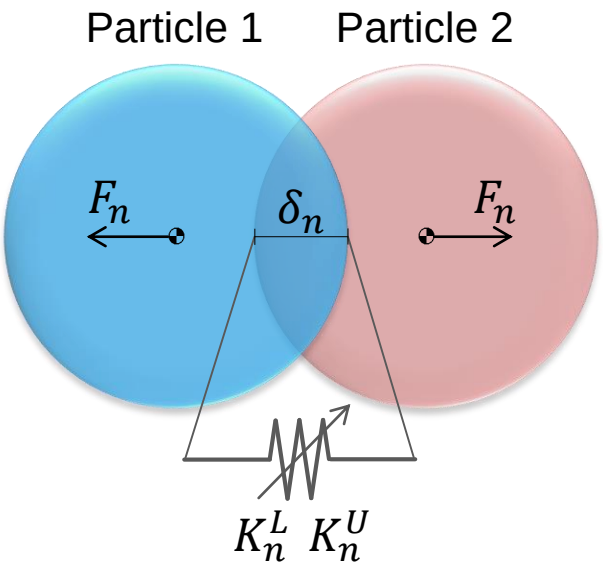

Force on particle 1: $\{F_n\} = -F_n^{el}\hat{n}$

$$F_n^{el} = \begin{cases} K_n^L \delta_n & \text{if} \quad \dot{\delta}_n \geq 0 \\ K_n^U \ (\delta_n - \delta_n^{res}) & \text{if} \quad \dot{\delta}_n < 0, \delta_n > \delta_n^{res} \\ 0 & \text{if} \quad \dot{\delta}_n < 0, \delta_n \leq \delta_n^{res} \end{cases}$$

- K_n^L → Loading spring stiffness
- K_n^U → Unloading spring stiffness ($K_n^U \geq K_n^L$)
- δ_n^{res} → Residual overlap

*Proposed by Walton & Braun (1986)

Elastic Perfectly Plastic Model

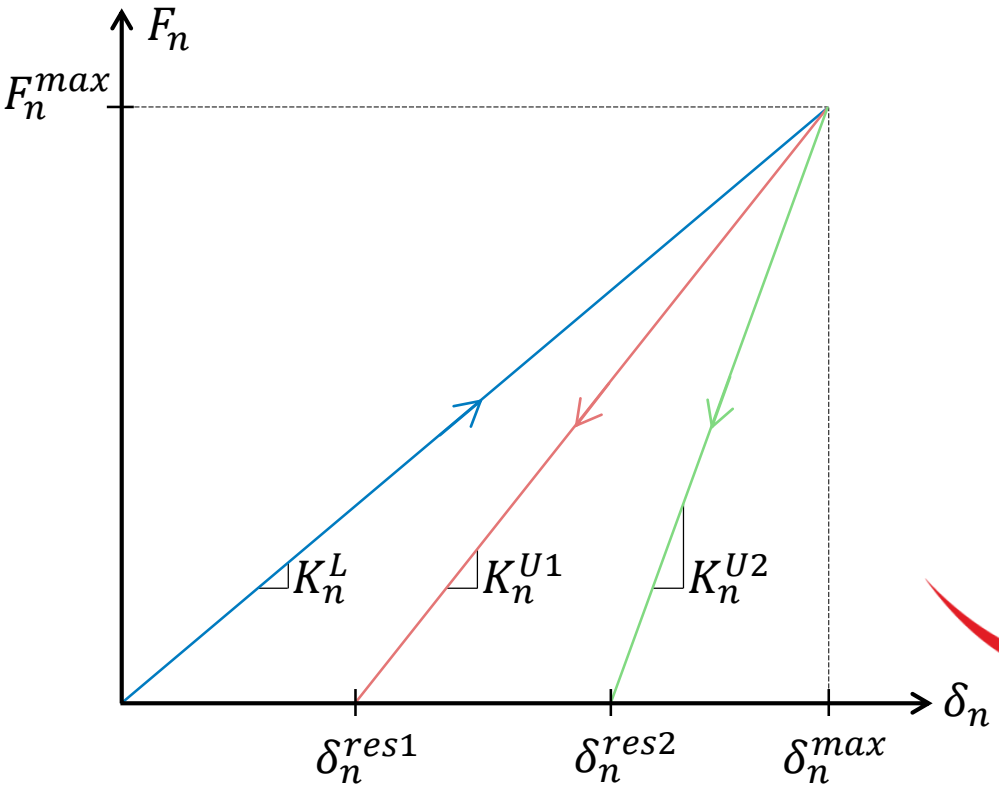

The restitution coefficient is related to the ratio between loading and unloading stiffness as:

$$\varepsilon_n = \sqrt{\frac{K_n^L}{K_n^U}}$$

$$\begin{cases} K_n^{U1} < K_n^{U2} \\ \varepsilon_{n1} > \varepsilon_{n2} \end{cases}$$

The loading path is always the same regardless of the restitution coefficient.

The residual overlap represents a permanent plastic deformation.

The energy dissipated during contact is the area between loading and unloading paths.

After full unloading, the residual deformation is forgotten for the next collisions.

Elastic Perfectly Plastic Model

Collision duration:

$$T_c = \frac{\pi}{2}\sqrt{\frac{\bar{m}}{K_n^L}}(\varepsilon_n + 1)$$

Maximum overlap:

$$\delta_n^{max} = \dot{\delta}_n^0 \sqrt{\frac{\bar{m}}{K_n^L}}$$

Residual overlap:

$$\delta_n^{res} = \delta_n^{max}\left(1 - \frac{K_n^L}{K_n^U}\right) = \dot{\delta}_n^0 \sqrt{\frac{\bar{m}}{K_n^L}}(1 - (\varepsilon_n)^2)$$

Maximum force:

$$F_n^{max} = K_n^L \dot{\delta}_n^0 \sqrt{\frac{\bar{m}}{K_n^L}}$$

Loading spring stiffness:

As with the LSDn model, 3 methods will be presented, each one sets a particular parameter equal to the result obtained with the NSDn model.

1) Equivalent Collision Duration:

$$K_n^L \cong 0.2996\left(\dot{\delta}_n^0 \bar{R}\bar{E}^2\sqrt{\bar{m}}\right)^{2/5}(\varepsilon_n + 1)^{\,2}$$

2) Equivalent Maximum Overlap:

$$K_n^L \cong 1.053\left(\dot{\delta}_n^0 \bar{R}\bar{E}^2\sqrt{\bar{m}}\right)^{2/5}$$

3) Equivalent Maximum Strain Energy:

$$K_n^L \cong 1.053\left(\dot{\delta}_n^0 \bar{R}\bar{E}^2\sqrt{\bar{m}}\right)^{2/5}$$

Elastic Perfectly Plastic Model

Constant unloading spring stiffness:

Assumes a constant unloading stiffness value, regardless of the maximum force, and thus a constant restitution coefficient.

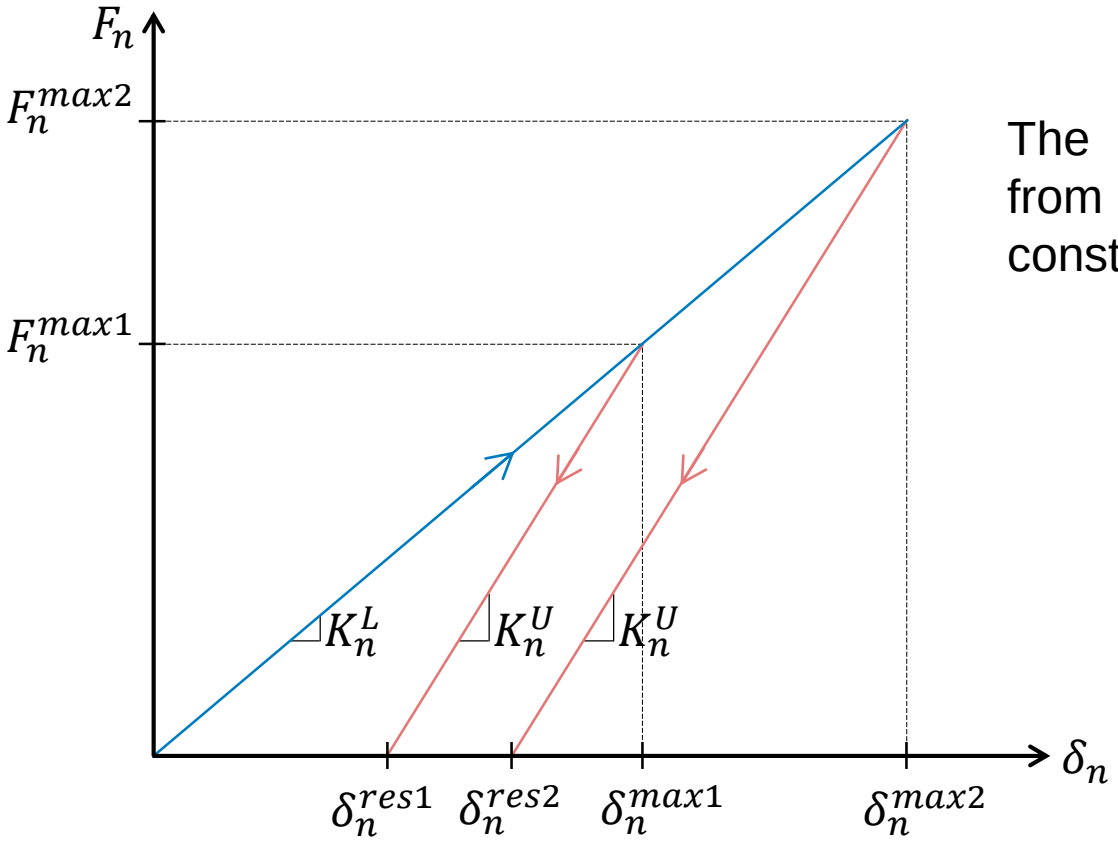

The unloading stiffness is obtained from the loading stiffness and a given constant restitution coefficient:

$$\varepsilon_n = \sqrt{\frac{K_n^L}{K_n^U}} \rightarrow K_n^U = \frac{K_n^L}{(\varepsilon_n)^2}$$

Elastic Perfectly Plastic Model

Variable unloading spring stiffness:

The unloading stiffness assumes different values depending on the maximum force, which results in a variable restitution coefficient.

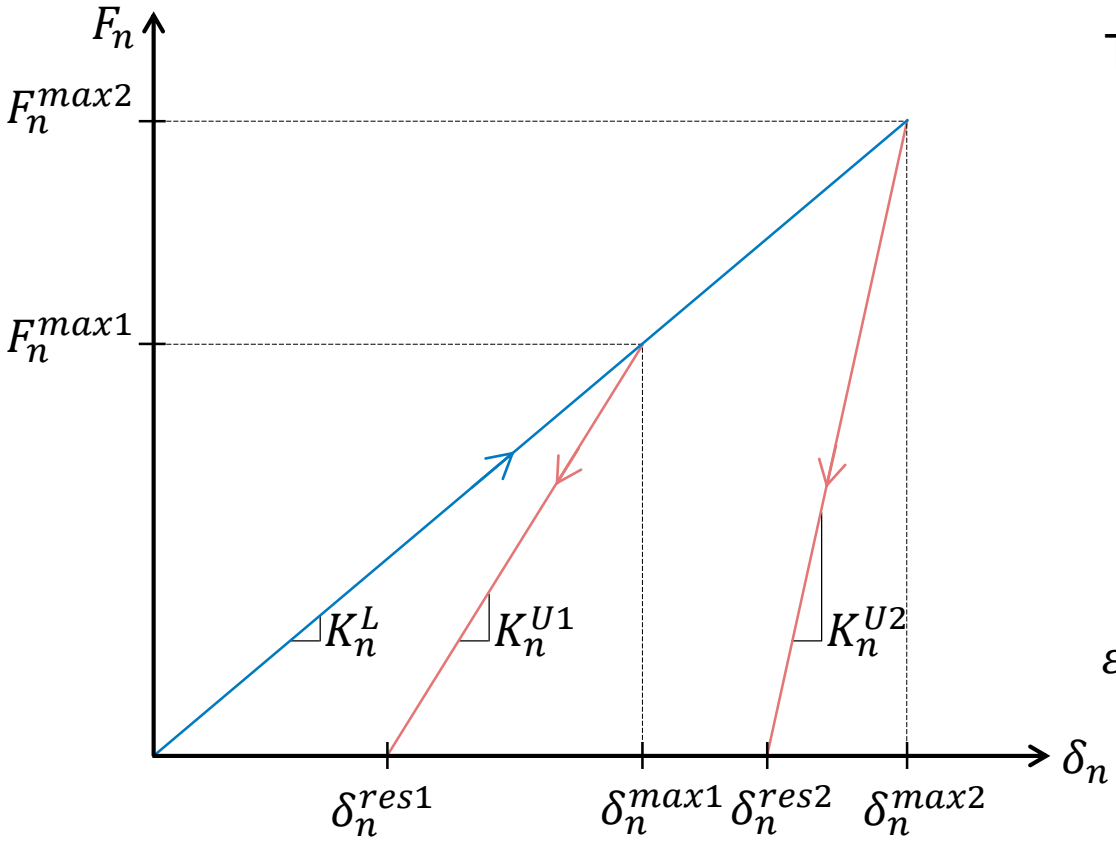

The unloading stiffness is given by:

$$K_n^U = K_n^L + SF_n^{max}$$

where the *S* can be determined empirically from experiments.

Applying the expression of K_n^U to the restitution coeff., it becomes a function of the impact velocity:

$$\varepsilon_n = \sqrt{\frac{K_n^L}{K_n^L + SF_n^{max}}} = \sqrt{\frac{1}{1 + S\dot{\delta}_n^0 \sqrt{\frac{\bar{m}}{K_n^L}}}}$$

Elastic Perfectly Plastic Model

Remarks on the HLS model:

- **Dependency on impact velocity**:
  In the constant unloading stiffness, as in the LSDn model, the restitution coefficient and collision duration are independent of the impact velocity.
  In the variable unloading stiffness, as in real collisions, the restitution coefficient and collision duration are an inverse function of the impact velocity
  (the former matches experimental data reasonably well while the later doesn't).

- **Continuous force:**
  The normal force is zero at the start / end of contact.

- **Cohesive force:**
  Differently from the viscoelastic models presented, the force is always repulsive and no reduction of contact time is needed.

- **Parameters behavior**:
  $T_c \uparrow$ as $K_n^L \downarrow$, $\overline{m} \uparrow$, $\varepsilon_n \uparrow$ (Directly proportional to ε_n, opposite to LSDn model)
  $\delta_n^{max} \uparrow$ as $K_n^L \downarrow$, $\overline{m} \uparrow$, $\dot{\delta}_n^0 \uparrow$ (Independent of ε_n, unlike in the LSDn model)

Summary of Normal Forces

Viscoelastic $\{F_n\} = -\left(F_n^{el} + F_n^{vis}\right)\hat{n}$

Linear

$F_n^{el} = K_n \delta_n \rightarrow K_n \cong 1.053\left(\dot{\delta}_n^0 \bar{R} \bar{E}^2 \sqrt{\bar{m}}\right)^{2/5}$ (Equivalent maximum strain energy)

$F_n^{vis} = \eta_n \dot{\delta}_n \rightarrow \eta_n = -\frac{2\ln(\varepsilon_n)\sqrt{\bar{m} K_n}}{\sqrt{\ln(\varepsilon_n)^2 + \pi^2}}$

Nonlinear

$F_n^{el} = K_{HZ} {\delta_n}^{3/2} \rightarrow K_{HZ} = \frac{4}{3}\bar{E}\sqrt{\bar{R}}$

$F_n^{vis} = \eta_n (\delta_n)^{1/4} \dot{\delta}_n \rightarrow \eta_n = -2.2664 \frac{\ln(\varepsilon_n)\sqrt{\bar{m} K_{HZ}}}{\sqrt{(\ln(\varepsilon_n))^2 + 10.1354}}$

(TTIn model)

(Poschel & Schwager, 2005)

Elastic Perfectly Plastic $\{F_n\} = -F_n^{el}\hat{n} \rightarrow F_n^{el} = \begin{cases} K_n^L \delta_n & \text{if} \quad \dot{\delta}_n \geq 0 \\ K_n^U \left(\delta_n - \delta_n^{res}\right) & \text{if} \quad \dot{\delta}_n < 0 \end{cases}$

$K_n^L \cong 1.053\left(\dot{\delta}_n^0 \bar{R} \bar{E}^2 \sqrt{\bar{m}}\right)^{2/5}$

Constant: $K_n^U = \frac{K_n^L}{(\varepsilon_n)^2}$

Variable: $K_n^U = K_n^L + S F_n^{max}$

Time reduction: $F_n^{el} + F_n^{vis} \geq 0$

4 – Tangential Force

Tangential Force

The tangent component of contact forces appears in oblique collisions due to surface friction between particles since the texture is never perfect but has small asperities.

Surface roughness allows a heap of sphere particles to be built on a flat surface

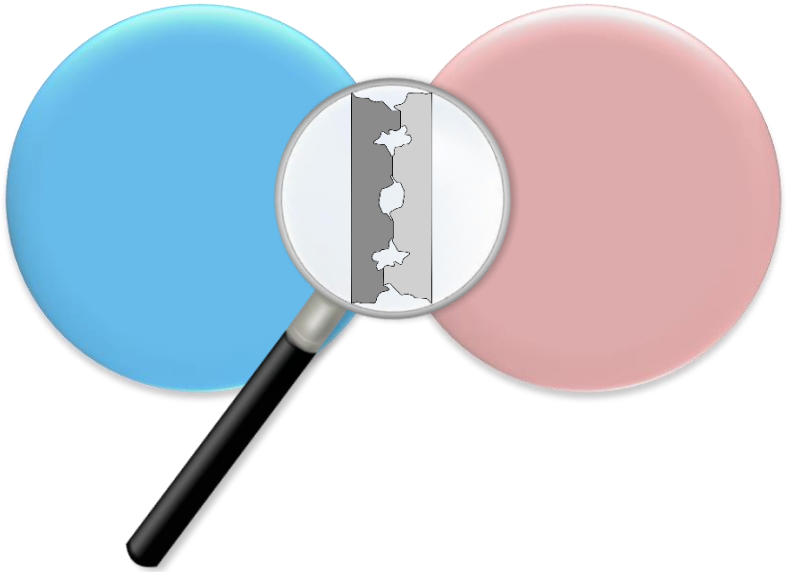

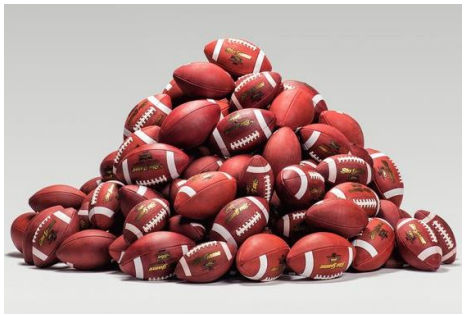

Non-spherical shapes may be more appropriate for static granular systems in which the tangent force is velocity-dependent

To take into account the surface roughness, tangent force models usually incorporate parameters that cannot be derived from basic material properties nor experiments, but only by adjusting simulation results with experimental data.

Coulomb's Law of Friction

The surface friction between particles is well modeled by Coulomb's law of friction.

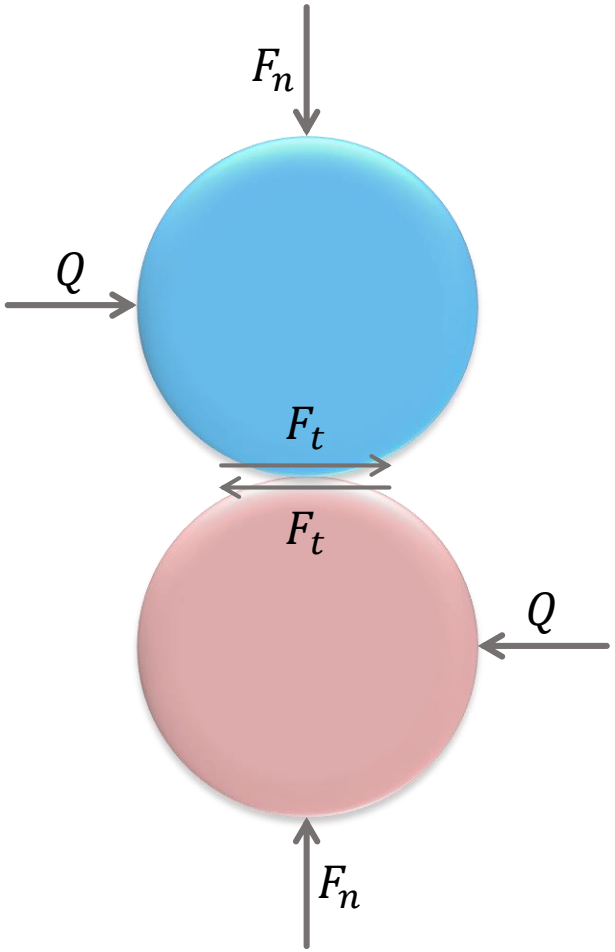

$$F_t = \begin{cases} Q & \text{if} \quad Q < \mu_s F_n \\ \mu_k F_n & \text{if} \quad Q \geq \mu_s F_n \end{cases}$$

μ_s → Static friction coeff.

μ_k → Kinetic friction coeff.

$(1 > \mu_s > \mu_k > 0.1)$

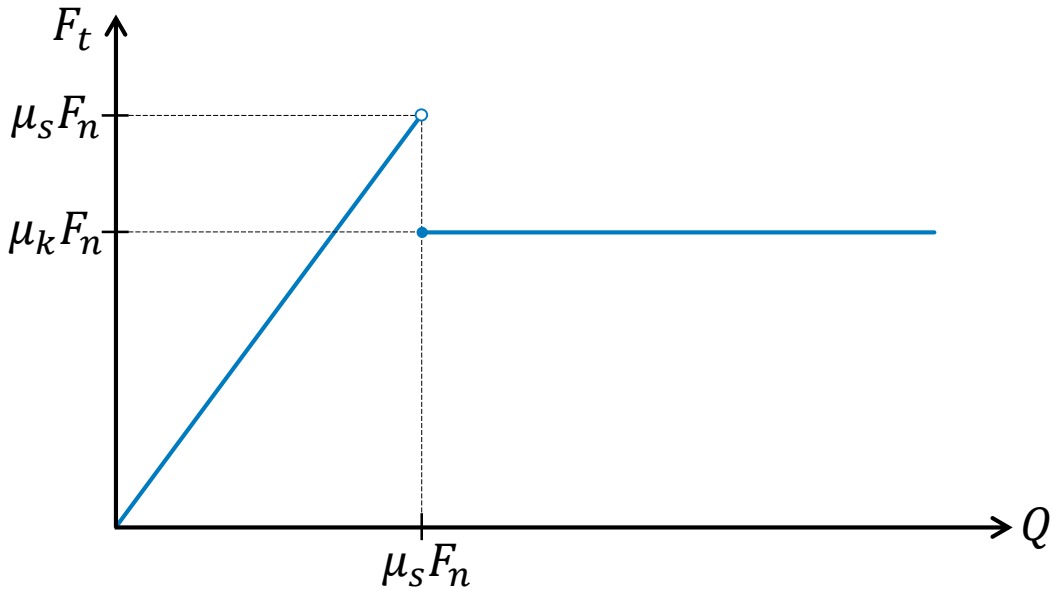

For low shear forces, there is no relative motion (stick)

For high shear forces, there is a relative motion (slip – gross sliding)

Coulomb's Law of Friction

In the tangent contact models, a single friction coefficient μ is usually considered.

If Coulomb's criterion is violated ($|Q| \geq \mu|F_n|$), gross sliding occurs and a slider is activated, in series with other mechanical elements, to provide the friction force.

The total force provided by other mechanical elements (say Q) never exceeds the friction force.

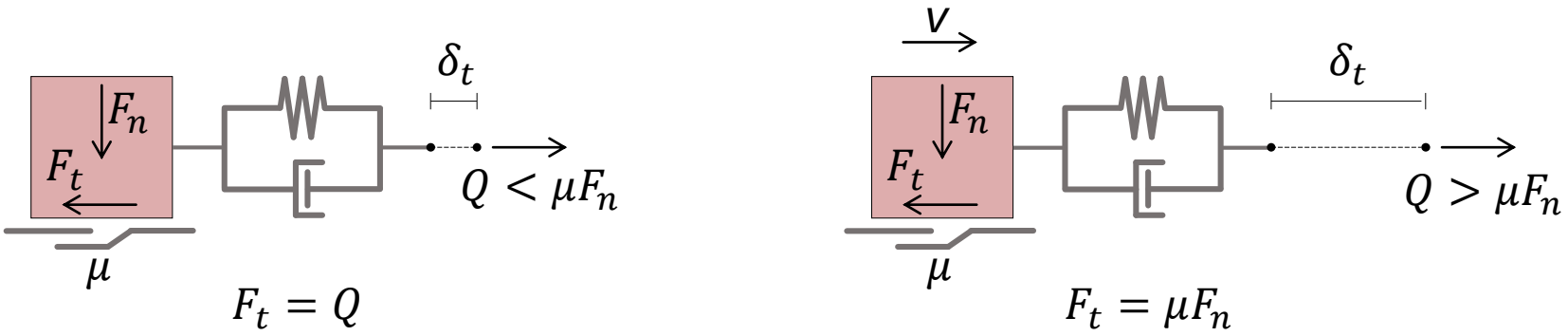

Therefore, the most common way to apply Coulomb's law is to limit the tangential force to the friction force provided by the slider (Cundall & Strack, 1979):

$$F_t = \min(|Q|, \mu|F_n|)$$

Coulomb's Law of Friction

Friction coefficients for the contact between materials (Wassgren & Sarkar, 2008):

Materials	Friction coefficient (μ)
soda lime glass / soda lime glass	0.092 ± 0.006
"fresh" glass / "fresh" glass	0.048 ± 0.006
"spent" glass / "spent" glass	0.177 ± 0.020
cellulose acetate / cellulose acetate	0.250 ± 0.020
nylon / nylon	0.175 ± 0.100
acrylic / acrylic	0.096 ± 0.0006
polystyrene / polystyrene	0.189 ± 0.009
stainless steel / stainless steel	0.099 ± 0.008
acrylic / aluminum plate	0.140
radish seeds / aluminum plate	0.190
"fresh" glass / aluminum plate	0.131 ± 0.007
"spent" glass / aluminum plate	0.126 ± 0.009
glass plate / glass plate	0.400
glass plate / nickel plate	0.560
glass plate / carbon plate	0.180

The friction coefficient of a material is given considering the contact of two surfaces of the same material; for two particles with different materials, the friction coefficient, when unknown, is taken as the minimum one, as proposed by Poschel & Schwager (2005).

Tangential Kinematics

Complementing the kinematics of motion previously presented here.

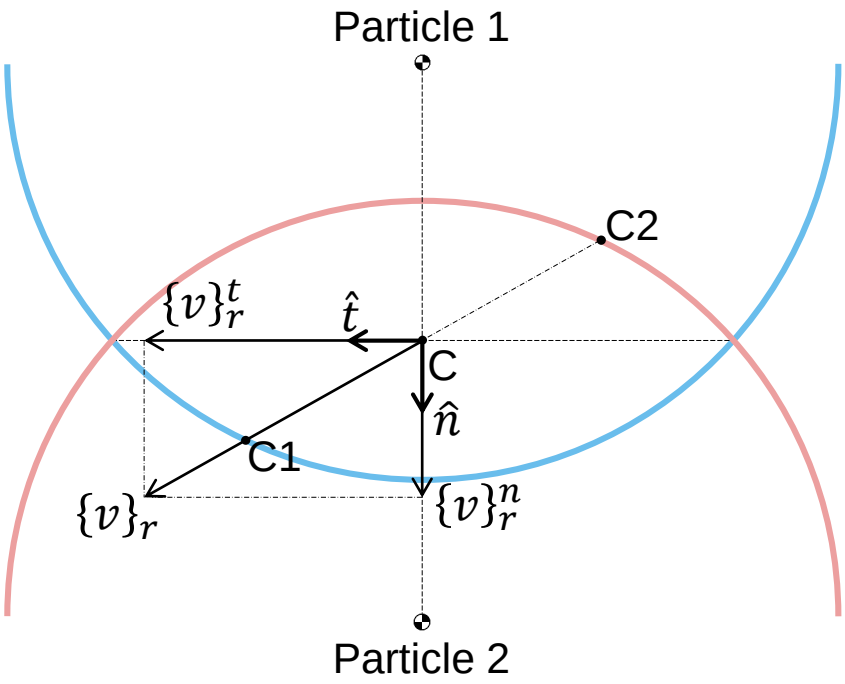

C → Current idealized contact point

C1 → Initial contact point of particle 1

C2 → Initial contact point of particle 2

The tangential direction $\hat{t}$ points towards the relative tangential velocity direction.

The tangential forces acts against the motion, therefore the force acting on particle 1 (reference particle throughout the presentation) is:

$$\{F_t\} = -F_t\hat{t}$$

Simple Sliding Friction

A slider is used to incorporate only the sliding friction.

It does not account for tangential deformation.

The force is always constant and changes only its direction.

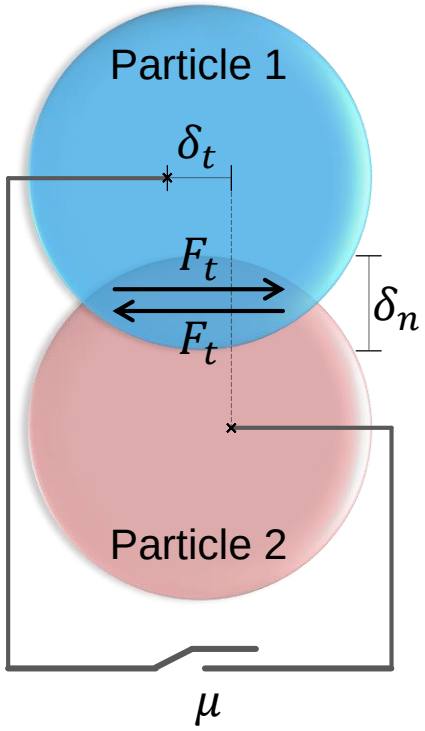

$F_t = \mu|F_n|$

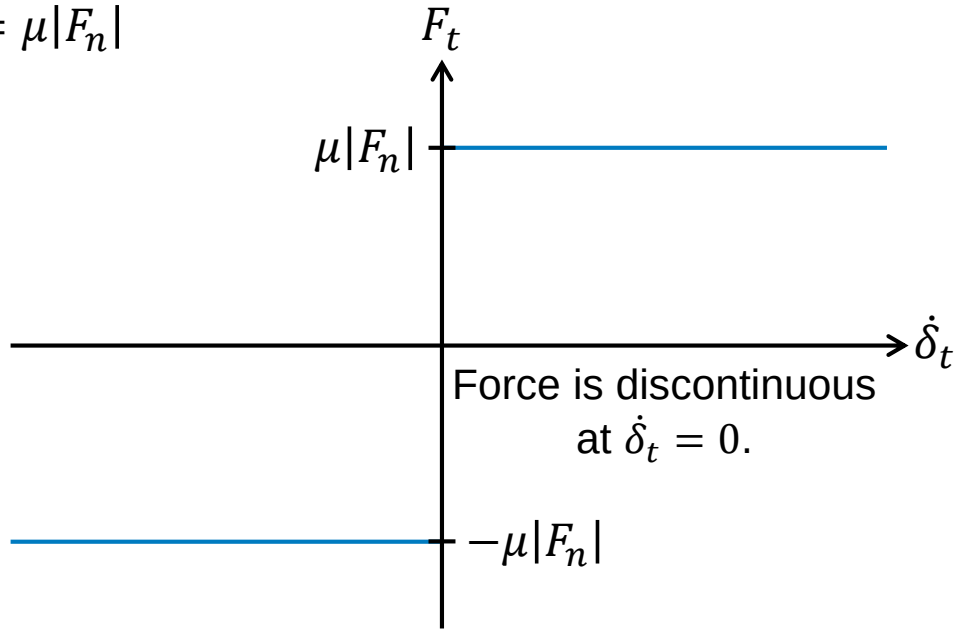

Simple Viscous Damping

A dashpot is used to incorporate only viscous force (η_t → tangential damping coeff.).

It does not account for tangential deformation nor sliding friction.

No dependency on normal force leads to poor behavior for grazing impacts.
It is physically justified for lubricated contacts.

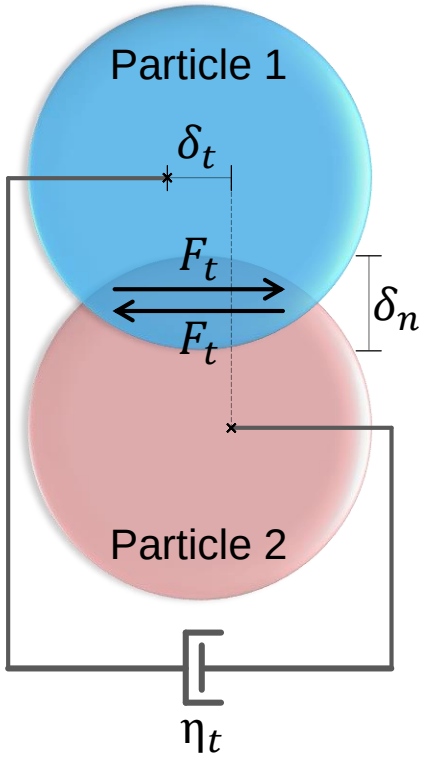

$$F_t = \eta_t \dot{\delta}_t$$

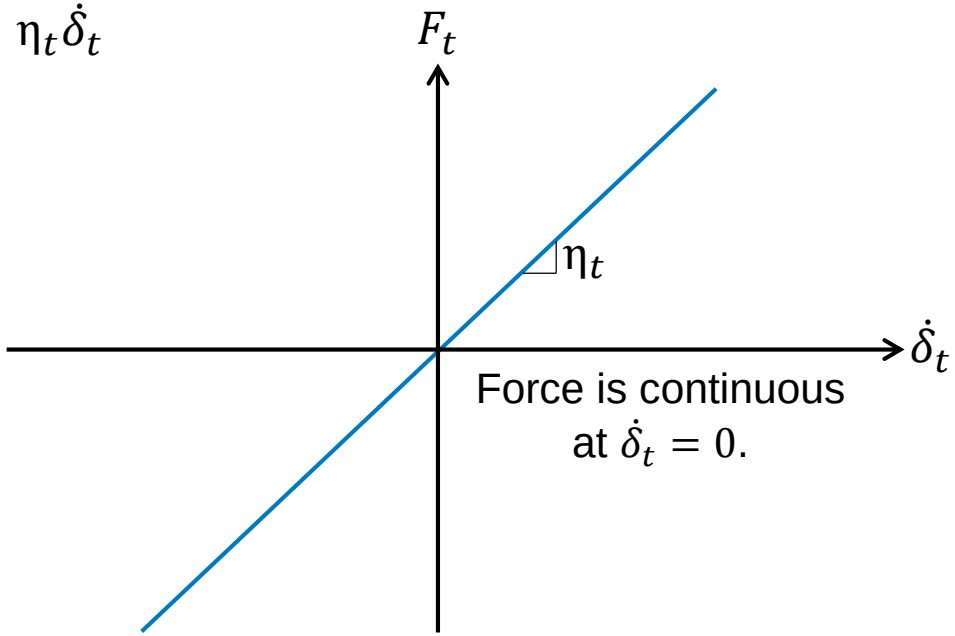

Viscous Damping with Sliding Friction

A dashpot is used to incorporate a viscous force, which is limited by Coulomb's law (combination of previous models).

It does not account for tangential deformation.

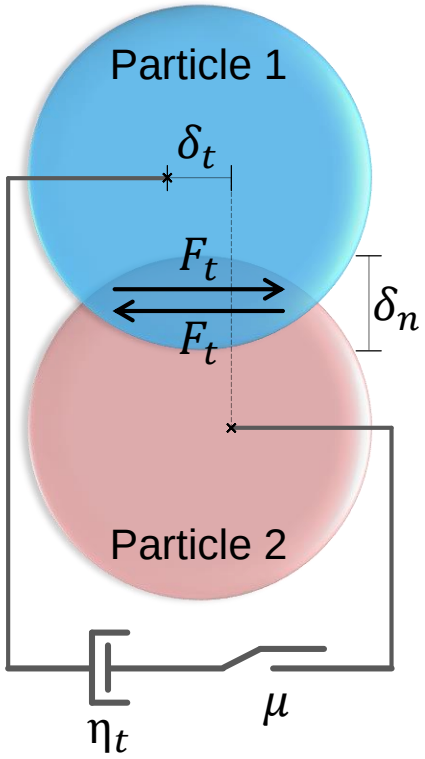

$$F_t = \min\left(\left|\eta_t \dot{\delta}_t\right|, \mu|F_n|\right)$$

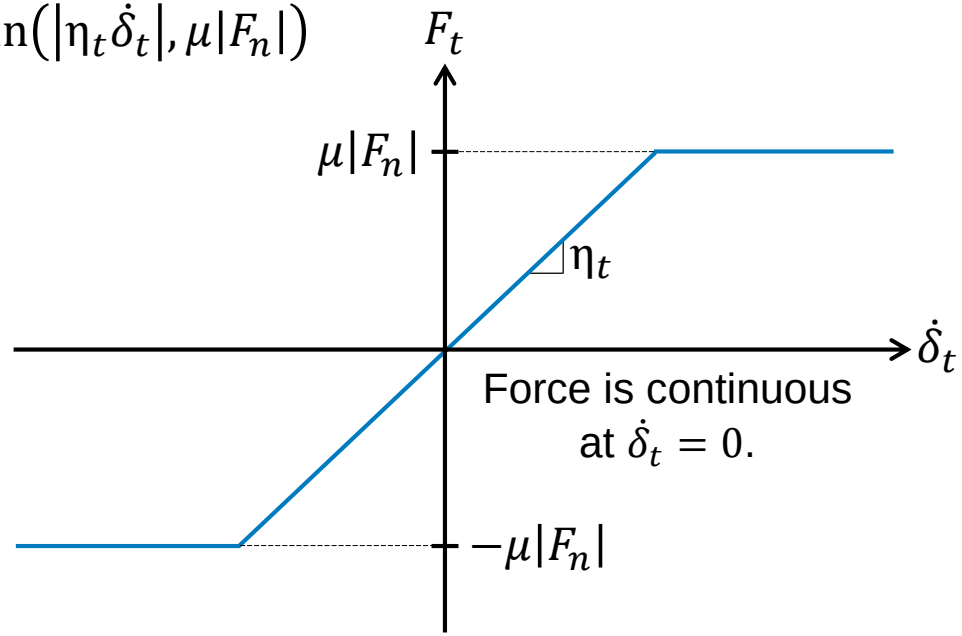

*Proposed by Haff & Werner (1986)

Viscous Damping with Sliding Friction

Remarks:

For a small tangential velocity or a large normal force, the tangential force is a shear damping that grows linearly with the velocity; For a large tangential velocity or a small normal force, the sliding friction force is selected.

Gives reliable results in systems where particles collide and do not rest statically at each other (e.g. a sand heap). Also appropriate for lubricated contact.

Problems appear in static systems when the relative velocities, and hence the tangential force, vanish since the model does not incorporate static friction. Therefore, this model is not suited for the simulation of static granular systems (a heap of such particles dissolves slowly).
A solution for this problem is to choose more complicatedly shaped particles.

A further problem concerns the damping coefficient. The tangential force is mainly determined by surface properties, i.e., by very small asperities at the particle surface. Therefore, there is no experimentally measurable material constant from which this coefficient could be derived. Instead this coefficient can only be determined à posteriori from the comparison of simulation results with experiments.

Linear Spring with Sliding Friction

A linear tangential spring is used to incorporate a elastic force of static friction (K_t → tangential spring stiffness), which is limited by Coulomb's law.

It does not depend on velocity and provides good results for static behavior.

The spring stiffness is determined by comparing simulation results with experiments.

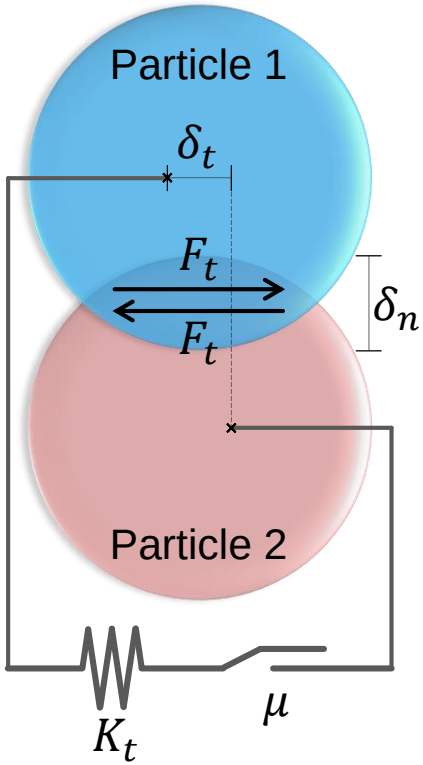

$$F_t = \min(|K_t \delta_t|, \mu |F_n|)$$

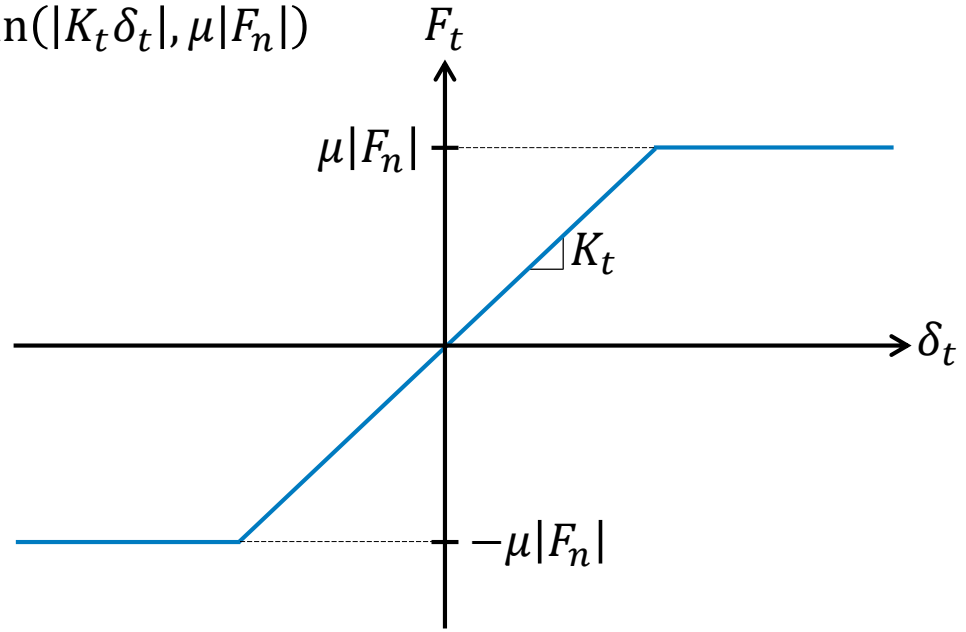

Dynamics of impact is governed by the ratio of tangent to normal stiffness: Normal spring sets the contact duration while tangent response is a function of the tangent spring stiffness.

*Proposed by Cundall & Strack (1979)

Linear Spring-Dashpot with Sliding Friction

A linear tangential spring and dashpot are used to incorporate viscoelastic forces, analogous to the LSDn model, but limited by Coulomb's law of friction.

It assumes no micro-slip in the contact area and constant spring stiffness.

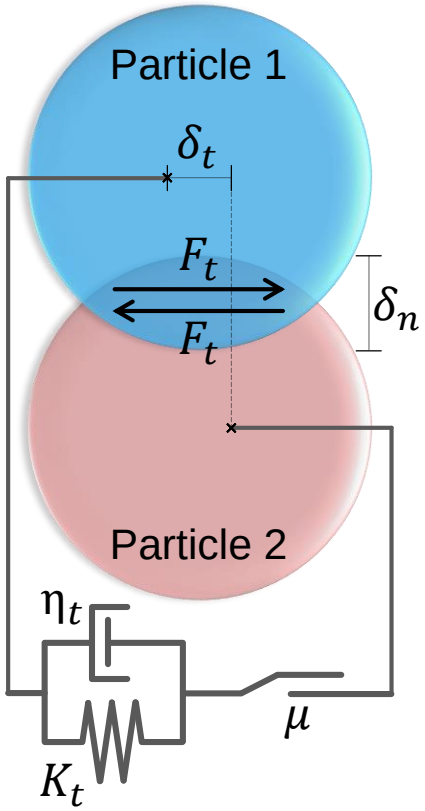

$$F_t = \min\left(\left|F_t^{el} + F_t^{vis}\right|, \mu|F_n|\right) \qquad \begin{cases} F_t^{el} = K_t \delta_t \\ F_t^{vis} = \eta_t \dot{\delta}_t \end{cases}$$

When slip occurs, the spring extension is adjusted to a value such that spring force matches friction force. Hence, another way to apply Coulomb's law is to limit the tangential overlap when gross sliding occur (Maw et. al, 1976). This limited overlap can provide better estimation of experimental data:

$$\delta_t = \text{sign}(\delta_t)\frac{\mu|F_n| - \eta_t \dot{\delta}_t}{K_t}$$

Then F_t is re-computed as $F_t^{el} + F_t^{vis}$.

Linear Spring-Dashpot with Sliding Friction

Spring stiffness:

It is common to set the tangential stiffness from the ratio between normal and tangential stiffness. From the elastic solid mechanics analysis of Mindlin (1949):

$$\frac{K_t}{K_n} = \frac{1-\nu}{1-\nu/2}$$

For common values of Poisson ratio: $(0 < \nu < 0.5)$

$$\frac{2}{3} < \frac{K_t}{K_n} < 1$$

Damping coefficient:

The value of the damping coefficient can only be determined by comparing results of simulation and experiments.

An expression was provided by Deen et. al (2007), based on the tangent coefficient of restitution (ε_t, obtained experimentally). This relation was obtained analytically, similarly to the expression of the LSDn model:

$$\eta_t = \begin{cases} -\dfrac{2\ln(\varepsilon_t)\sqrt{2/7\,\bar{m}K_t}}{\sqrt{\ln(\varepsilon_t)^2+\pi^2}} & \text{if} \quad \varepsilon_t \neq 0 \\ 2\sqrt{2/7\,\bar{m}K_t} & \text{if} \quad \varepsilon_t = 0 \end{cases}$$

Cundall & Strack (1979) set the tangential damping coefficient to be proportional to the tangential spring stiffness.

Nonlinear Spring-Dashpot with Sliding Friction

Nonlinear version of previous model and analogous to the NSDn model, but again limited by Coulomb's law of friction.

There are many ways to set the spring stiffness and the damping coefficient, some of them are presented in the following.

1) DDt model (Di Renzo & Di Maio, 2005):

$$F_t^{el} = K_t \delta_t \qquad K_t = \frac{16}{3} \bar{G} \sqrt{\bar{R} \delta_n}$$

Micro-slip conditions on the contact area and variable normal force on the contact surface are approximately considered.

Unlike the linear model, the nonlinear spring stiffness is continuously changing during a collision because the normal overlap is not constant.

This model does not consider viscous force. However, it can be incorporated by a damping force proportional to the velocity similar to the linear model.

Nonlinear Spring-Dashpot with Sliding Friction

2) LTH model (Langston et. al, 1994):

Simplified model for a contact with constant normal force.

Ensures that gross sliding occurs when tangent displacement is greater than the displacement in which sliding starts (δ_t^{max}):

$$\delta_t^{max} = \mu \frac{(2-\nu)}{2(1-\nu)} \delta_n$$

$$F_t^{el} = \mu |F_n| \left(1 - \left(1 - \frac{\min(|\delta_t|, \delta_t^{max})}{\delta_t^{max}} \right)^{3/2} \right)$$

$$F_t^{vis} = \eta_t \left(\frac{6\bar{m}\mu|F_n| \sqrt{1 - \frac{\min(|\delta_t|, \delta_t^{max})}{\delta_t^{max}}}}{\delta_t^{max}} \right)^{1/2} \dot{\delta}_t$$

Nonlinear Spring-Dashpot with Sliding Friction

3) ZZYt model (Zheng et. al, 2012):

The elastic force is computed as in model 2, but the viscous force is computed in an improved way:

$$F_t^{vis} = \frac{\eta_1}{2G_i\delta_t^{max}}\left(1 - \frac{0.4\eta_1|\dot{\delta}_t|}{2G_i\delta_t^{max}}\right)\left(1.5\mu|F_n|\sqrt{1 - \frac{\min(|\delta_t|, \delta_t^{max})}{\delta_t^{max}}}\right)\dot{\delta}_t$$

4) TTIt model (Tsuji et. al, 1992):

A tangential stiffness was derived from the no-slip solution of Mindlin (1949), assuming a damped Hertz normal spring force and constant coefficient of restitution.
The tangential damping coefficient is set equal to the normal damping coefficient.

$$F_t^{el} = K_t\delta_t \qquad K_t = \frac{\sqrt{2R}E}{(2-\nu)(1+\nu)}\sqrt{\delta_n}$$

Incrementally Slipping Friction

Complementary to the HLS model in normal force: a hysteric spring with different loading and unloading stiffness provides an elastic force limited by Coulomb's law.

More sophisticated: It is not only determined by the particle positions and velocities at the present time, but also depends on the history of the interaction.

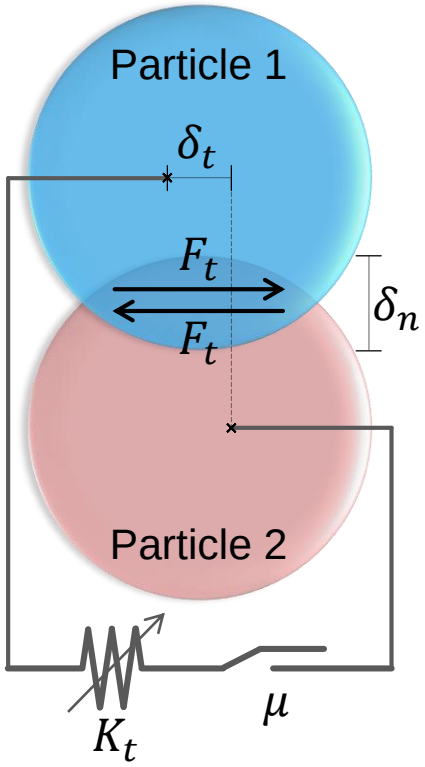

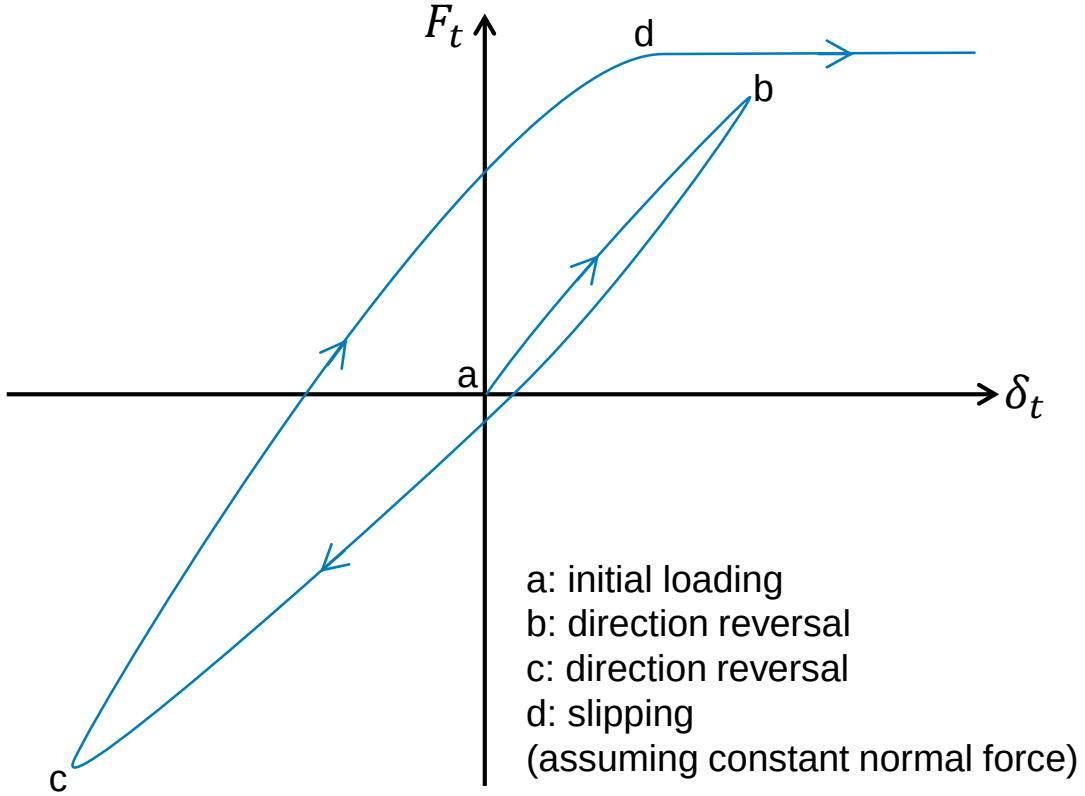

*Proposed by Walton & Braun (1986)

Incrementally Slipping Friction

The tangential force is computed incrementally: the force at a time step *T2* is obtained from the force at time step *T1* plus an increment of force associated to an increment of tangential overlap ($\Delta\delta_t$):

$$F_t^{T2} = F_t^{T1} + K_t \Delta\delta_t$$

When particles collide at certain angle, they begin to slide against each other and the tangential force increases with the spring elongation, limited by Coulomb's law.
If the particles begin to slide in the opposite direction (direction reversal), the tangential force decreases, but with a different path.

After direction reversal, the spring stiffness assumes a different value, such that Coulomb's law is enforced ($K_t = 0$ when $F_t^{T1} = \mu F_n$) and depends on the initial stiffness value (K_t^0) and on the tangent force when the last slipping reversal occurred (F_t^* → initially 0):

$$K_t = sK_t^0 \left(1 - \frac{F_t^{T1} - F_t^*}{\mu F_n - sF_t^*}\right)^{1/3} \qquad s = \begin{cases} 1 & \text{If } \dot{\delta}_t \text{ is in the initial direction (slipping increases } F_t^{T1}) \\ -1 & \text{If } \dot{\delta}_t \text{ is in the opposite direction (slipping decreases } F_t^{T1}) \end{cases}$$

Incrementally Slipping Friction

Remarks:

- Assumes that normal the normal force remains constant between time steps (justified for a gradually changing normal force).
- The difference of the tangent stiffness of loading and unloading paths is the source of energy dissipation.
- For implementation, it needs to store some information of the contact history.
- Extension to 3D is complicated because of the definition of a direction reversal.

Nomenclature & Bibliography

Nomenclature

Geometric and Physical Properties

R_i	Radius of particle *i*
$\bar{R}$	Effective radius of two particles
m_i	Mass of particle *i*
$\bar{m}$	Effective mass of two particles
E_i	Young modulus of particle *i*
$\bar{E}$	Effective Young modulus of two particles
G_i	Shear modulus of particle *i*
$\bar{G}$	Effective shear modulus of two particles
A_i	Dissipative constant
$\bar{A}$	Effective dissipative constant of two particles
ν_i	Poisson ratio of particle *i*
ε_n, ε_t	Normal / tangential coefficient of restitution

Kinematics

X, Y, Z, r	Cartesian and radial coordinate systems
d	Distance between center of two particles
δ_n, δ_t	Normal / tangential overlap
δ_n^{max}, δ_t^{max}	Maximum normal / tangential overlap
δ_n^{res}	Residual normal overlap
$\dot{\delta}_n$, $\dot{\delta}_t$	Normal / tangential relative velocity
$\dot{\delta}_n^0$, $\dot{\delta}_n^{reb}$	Normal relative velocity of Impact / rebound
$\ddot{\delta}_n$	Normal relative acceleration
h_0, h_{reb}	Height of drop / rebound in free-fall test
$\{x\}_i$	Position vector of center of particle *i*
$\{r\}_i$	Position vector from center of particle *i* to contact point
$\hat{n}$, $\hat{t}$	Normal / tangential unit vectors
$\{v\}_i$	Translational velocity vector at the center of particle *i*
$\{v\}_{ri}$	Translational velocity vector at the contact point of particle *i*
$\{v\}_r$	Translational velocity vector of particle 2 relative to particle 1 at contact point
$\{v\}_r^n$, $\{v\}_r^t$	Normal / tangential components of $\{v\}_r$
$\{\omega\}_i$	Rotational velocity vector of particle *i*

Forces

F	Generic force
M	Generic torque
F_C	Contact force
F_{NC}	Non-contact force
F_g	Gravitational force
F_f	Fluid force

Nomenclature

F_n, F_t	Normal / tangential component of contact force
F_n^{el}, F_t^{el}	Elastic normal / tangential force
F_n^{vis}, F_t^{vis}	Viscous normal / tangential force
F_n^{max}	Maximum normal force
F_n^T, F_t^T	Normal / tangential force at time step *T*
F_t^*	Tangent force at the last slipping reversal

Model Parameters

K_n, K_t	Normal / tangential spring stiffness
K_{HZ}	Hertzian normal spring stiffness
K_n^L, K_n^U	Loading / unloading normal spring stiffness
K_n^0, K_t^0	Initial normal / tangential stiffness value
η_n, η_t	Normal / tangential damping coefficient
μ_s	Static friction coefficient
μ_k	Kinetic friction coefficient
μ	General Coulomb friction coefficient

Others

Δ	Time step increment of a variable
T	Generic time
T_c	Collision duration
P	Normal stress distribution on collision contact area
P_{max}	Maximum value of normal stress distribution
a	Radius of collision contact area
S	Variable unloading stiffness parameter
Q	Generic shear force
Ψ, Φ, W, β	Auxiliary parameters

Bibliography

1. Brilliantov, N.V., Spahn, F., Hertzsch, J.-M., and Poschel, T. A model for collisions in granular gases. *Phys. Rev. E*, 53:5382, 1996.
2. Cundall, P.A., and Strack, O.D.L. A discrete numerical model for granular assemblies. *Geotechnique*, 29, 47-65, 1979.
3. Deen, N.G., Van Sint Annaland, M., Van der Hoef, M.A., and Kuipers, J.A.M. Review of discrete particle modeling of fluidized beds. *Chemical Engineering Science*, 62, 28-44, 2007.
4. Di Renzo, A. and Di Maio, F.P. An improved integral non-linear model for the contact of particles in distinct element simulations. *Chemical Engineering Science*, 60, 1303-1312, 2005.
5. Haff, P.K., and Werner, B.T. Computer simulation of the mechanical sorting of grains. *Powder Techn.*, 48, 239-245, 1986.
6. Hertz, H. Uber die Beruhrung fester elastischer Korper. *J. f. reine u. Angewandte Math.*, 92, 156-171, 1882.
7. Johnson, K.L. *Contact Mechanics*. Cambridge University Press, 1985.
8. Kuwabara, G., and Kono, K. Restitution coefficient in collision between two spheres. *Japanese Journal of Applied Physics*, 26, 1230-1233, 1987.
9. Kruggel-Emden, H., Wirtz, S., and Scherer, V. A study on tangential force laws applicable to the discrete element method (DEM) for materials with viscoelastic or plastic behavior. *Chemical Engineering Science*, 63, 1523-1541, 2008.
10. Langston, P.A., Tuzun, U., and Heyes, D.M. Continuous potential discrete particle simulations of stress and velocity-fields in hoppers-transition from fluid to granular flow. *Chemical Engineering Science*, 49, 1259-1275, 1994.
11. Maw, N., Barber, J.R., and Fawcett, J.N. The oblique impact of elastic spheres. *Wear*, 38, 101-114, 1976.
12. Mindlin, R.D. Compliance of Elastic Bodies in Contact. *Journal of Applied Mechanics*, 16, 259-268, 1949.
13. Norouzi, H.R., Zarghami, R., Sotudeh–Gharebagh, R., Mostoufi, N. *Coupled CFD–DEM Modeling: Formulation, Implementation and Application to Multiphase Flows*. Wiley, 2016.
14. Poschel, T., and Schwager, T. *Computational Granular Dynamics*. Springer, Berlin, 2005.
15. Tsuji, Y., Tanaka, T., and Ishida, T. Lagrangian numerical simulation of plug flow of cohesionless particles in a horizontal pipe. *Powder Technology*, 71, 239–250, 1992.
16. Walton, O.R., and Braun, R.L. Viscosity, granular temperature, and stress calculations for shearing assemblies of inelastic, frictional disks. *J. Rheol.*, 30:949, 1986.
17. Wassgren, C., and Sarkar, A. *Discrete Element Method (DEM) Course Module*, 2008. https://pharmahub.org/resources/113.
18. Zheng, Q.J., Zhu, H.P., and Yu, A.B. Finite element analysis of the contact forces between a viscoelastic sphere and rigid plane. *Powder Technology*, 226, 130-142, 2012.